

Ligand Control in Multihaptotropic O-Indenyl Rhenium Systems. Experimental and Theoretical Study

Silvia Bordoni,* Stefano Cerini, Riccardo Tarroni, Stefano Zacchini, and Luigi Busetto

*Dipartimento di Chimica Fisica ed Inorganica, Università di Bologna, Viale Risorgimento,
4 I-40136 Bologna, Italy*

Received May 20, 2009

The synthesis of a novel class of alcohol- and ether-functionalized indenyl ligands, focusing on the haptotropic rearrangements of the hybrid O-indenyl rhenium species, is herein described. η^1 -Ind_x^{OMe}Re(CO)₅ (**12_x**) and η^3 -Ind_x^{OMe}Re(CO)₄ (**13_x**, **x** = **a**, **d**) [**Ind_a**^{OMe} = C₉H₆CH₂CH(Me)OMe, **1a**; **Ind_d**^{OMe} = C₉H₆CH(CH₂)₃CHOMe, **1d_a**] are examples of σ and allylic intermediates in the Cp substitution. The tuning of stereoelectronic effects of the functionalized alkyl chain or the coordinating solvent (MeCN, THF) allows the study of the relative stabilities of the intercepted solvento species η^5 -Ind_b^{OMe}Re(CO)₂(NCMe), **14_b**, η^5 -Ind_c^{OMe}Re(CO)₂(THF), **15_c**, or the chelate [η^5 :*k*¹-O-Ind_{b,c}^ORe(CO)₂], **16_{b,c}** {**Ind_b**^{OMe} = [C₉H₆CH₂CH(Ph)OMe]⁻, **4_b**; **Ind_c**^{OMe} = [C₉H₆CH(Ph)CH₂OMe]⁻, **4_c**}. DFT calculations reported on some of the Ind^O systems have been compared with those of smaller (Cp^O) **5_a** or larger (Flu_a^O) **10_a** congeners, confirming the experimental findings. As peculiar examples of the underrepresented low-valent rhenium alkoxy species, the isolation of *k*¹-O-HInd_x^ORe(CO)₅ [**x** = **a**, **b**] is also reported.

Introduction

A great deal of attention has been devoted in the past decade¹ to hybrid ligands having polyene π -extended rings such as indenyl (Ind⁻) or fluorenyl (Flu⁻) with peripheral heteroatom-alkyl pendants, focusing on the excellent catalytic performances of their coordinated early transition metal in polymerization reactions.² The increased efficiency

of these versatile systems depends on the hemilabile donor atom's chelating aptitude and on their haptotropic flexibility.³ Particular efforts have been dedicated to exploiting features of amino- or phosphino-alkyl ligands⁴ in early (Ti, Zr)⁵ or mid-late (Mo, Fe, Ru, Rh)⁶ transition metal complexes. Although nucleophilic epoxide ring-opening constitutes an efficient method to associate oxygen functions to polyene systems,⁷ few examples are reported on the oxygen-functionalized Cp-like rhenium complexes.⁸

*Corresponding author. E-mail: silvia.bordoni@unibo.it.

(1) (a) Tellier, C.; Lelong, J.-F.; Huriez, E. *GWXXBX DE*; 10250062 A1, 2004. (b) Kim, E.-I.; Choi, S. D. *U.S. Pat. Appl. USXXCO US 2004054207 A1*, 2004. (c) Esteb, J. J.; Chien, J. C. W.; Rausch, M. D. *J. Organomet. Chem.* **2003**, *688*, 153. (d) Graf, D. D.; Soto, J. *PCT Int. Appl. WO 2003078483 A1*, 2003. (e) Mihan, S.; Lilge, D.; De Lange, P.; Schweier, G.; Schneider, M.; Rief, U.; Handrich, U.; Hack, J.; Enders, M.; Ludwig, G.; Rudolph, R. *PCT Int. Appl. WO 2001012641 A1*, 2001. (f) Müller, C.; Vos, D.; Jutzi, P. *J. Organomet. Chem.* **2000**, *600*, 127. (g) Butenschön, H. *Chem. Rev.* **2000**, *100*, 1527. (h) Siemeling, U. *Chem. Rev.* **2000**, *100*, 1495. (i) Ready, T. E.; Chien, J. C. W.; Rausch, M. D. *J. Organomet. Chem.* **1999**, *583*, 11. (j) Britovsek, G. J. P.; Gibson, V. C.; Waas, D. F. *Angew. Chem., Int. Ed.* **1999**, *38*, 428. (k) McKnight, A. L.; Waymouth, R. M. *Chem. Rev.* **1998**, *98*, 2587.

(2) (a) Leino, R.; Lehmus, P.; Lehtonen, A. *Eur. J. Inorg. Chem.* **2004**, 3201. (b) Graf, D. D.; Kuhlman, R. L. (Dow Global Technologies Inc.) *PCT Int. Appl. WO 2004013149 A1 20040212*, **2004**. (c) Royo, S. J.; Munoz-Escalona Lafuente, A.; Begona, P. G.; Carlos, M. M. (Repsol Química S.A.) *US 6635778; B1 20031021*, 2003. (d) Klosin, J.; Kruper, W. J.; Nickias, P. N.; Roof, G. R.; Soto, J.; Graf, D. D. (Dow Global Technologies Inc.) *U.S. Pat. Appl. US 2003004286; A1 20030102*, **2003**. (e) Graf, D. D.; Soto, J. (Dow Global Technologies Inc.) *PCT Int. Appl. WO 2003078483; A1 20030925*, 2003. (f) Arndt, S.; Beckerle, K.; Hultzsich, K. C.; Sinnema, P. J.; Voth, P.; Spaniol, T. P.; Okuda, J. *J. Mol. Catal. A: Chem.* **2002**, *190*, 215. (g) Altenhoff, G.; Bredeau, S.; Erker, G.; Kehr, G.; Kataeva, O.; Froehlich, R. *Organometallics* **2002**, *21*, 4084. (h) Kunz, K.; Erker, G.; Doering, S.; Froehlich, R.; Kehr, G. *J. Am. Chem. Soc.* **2001**, *123*, 6181. (i) Britovsek, G. J. P.; Gibson, V. C.; Wass, D. F. *Angew. Chem., Int. Ed.* **1999**, *38*, 428.

(3) Trifonov, A.; Ferri, F.; Collin, J. *J. Organomet. Chem.* **1999**, *582*, 211.

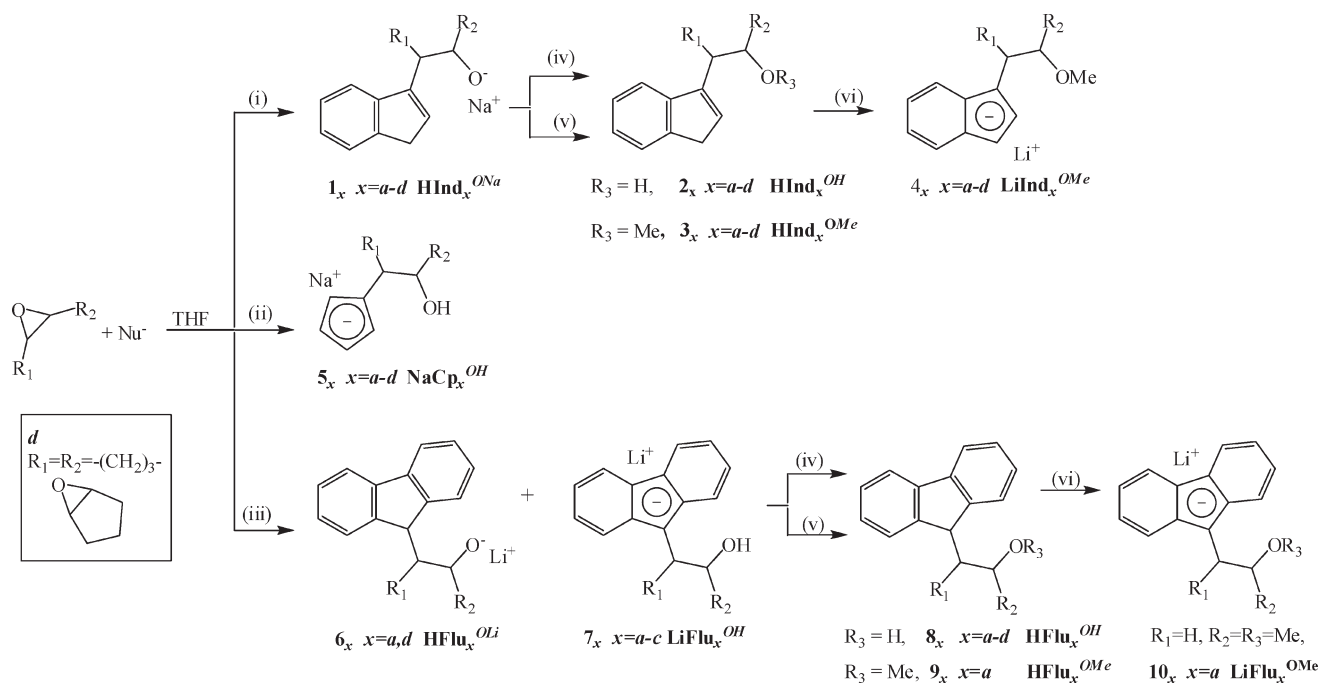
(4) (a) Esteruelas. *Organometallics* **2005** *24* 5084, and references therein. (b) Döhning, A.; Jensen, V. R.; Jolly, P. W.; Thiel, W.; Weber, J. C. *Organometallics* **2001**, *20*, 2234. (c) Doppiu, A.; Englert, U.; Salzer, A. *Inorg. Chim. Acta* **2003**, *350*, 435. (d) Bul, M. L.; Esteruelas, M. A.; López, A. M.; Mateo, A. C. *Organometallics* **2006**, *25*, 4079, and references therein.

(5) (a) Jany, G.; Fawzi, R.; Steimann, M.; Rieger, B. *Organometallics* **1997**, *16*, 544. (b) Rieger, B.; Jany, G.; Fawzi, R.; Steimann, M. *Organometallics* **1994**, *13*, 647. (c) Rieger, B.; Jany, G.; Steimann, M.; Fawzi, R. *Z. Naturforsch., B: Chem. Sci.* **1994**, *49*, 451. (d) Rieger, B.; Jany, G.; Fawzi, R.; Steimann, M. *Organometallics* **1994**, *13*, 647. (e) Rieger, B. *J. Organomet. Chem.* **1991**, *420*, C17.

(6) (a) Vogelgeasang, J.; Frick, A.; Huttner, G.; Kircher, P. *Eur. J. Inorg. Chem.* **2001**, 949. (b) Scherer, J.; Huttner, G.; Buchner, M.; Bakos, J. *J. Organomet. Chem.* **1996**, *520*, 45. (c) O'Connor, J. M.; Casey, C. P. *Chem. Rev.* **1987**, *87*, 307–318. (d) Brookings, D. C.; Harrison, S. A.; Whitby, R. J.; Crombie, B.; Jones, R. V. H. *Organometallics* **2001**, *20*, 4574.

(7) (a) Howell, F. H.; Taylor, D. A. H. *J. Chem. Soc.* **1957**, 3011. (b) Cuvigny, T.; Normant, H. *Bull. Soc. Chem. Fr.* **1964**, *5*, 2000. (c) Cagniant, P.; Merle, G.; Cagniant, D. *Bull. Soc. Chem. Fr.* **1970**, *1*, 308. (d) Ohta, H.; Kobori, T.; Fujisawa, T. *J. Org. Chem.* **1977**, *42*, 1231. (e) Kumamoto, T. *Bull. Chem. Soc. Jpn.* **1986**, *59*, 3097. (f) Perumattam, J.; Shao, C.; Confer, W. L. *Synthesis* **1994**, 1181. (g) Fuller, L. S.; Iddon, B.; Smith, K. A. *J. Chem. Soc., Perkin Trans. 1* **1997**, 3465. (h) Panarello, A. P.; Vassilyev, O.; Khinast, J. G. *Synlett* **2005**, 797–800. (i) Bordoni, S.; Natanti, P.; Cerini, S.; Tarroni, R.; Monari, M.; Piccinelli, F.; Busetto, L. *Organometallics* **2008**, *27*, 945–954.

(8) (a) Busetto, L.; Cassani, M. C.; Zanotti, V.; Albano, V. G.; Sabatino, P. *Organometallics* **2001**, *20*, 282–288. (b) Wang, T.; Hwu, C.; Tsai, C.; Wen, Y. *Organometallics* **1998**, *17*, 131.

Chart 1^a

^a Abbreviations and reaction conditions: Nu = C₅H₅ Cp; C₉H₇ Ind; C₁₃H₉ Flu. *a* R₁ = H, R₂ = Me; *b* R₁ = H, R₂ = Ph; *c* R₁ = Ph, R₂ = H; *d* R₁ = R₂ = -(CH₂)₃-; (i) rt for **1_{a,d}**; reflux for **1_{b,c}**; (ii) rt; (iii) -78 °C to rt; (iv) NH₄Cl(aq) for **2_{a-d}**, **8_{a-d}**; (v) toluene, MeOTf, -78 °C to rt; (vi) LiMe or LiBu, THF, -78 °C.

Herein we describe the syntheses of several indenyl hybrid ligands, Ind^O, with a two-carbon alkyl linker such as 2-methyl, Ind^{OMe}_a = [C₉H₆CH₂CH(Me)OMe]⁻, **1_a**; 2-phenyl, Ind^{OMe}_b = [C₉H₆CH₂CH(Ph)OMe]⁻, **1_b**; 1-phenyl, Ind^{OMe}_c = [C₉H₆CH(Ph)CH₂OMe]⁻, **1_c**, and cyclopentyl,

Ind^{OMe}_d = [C₉H₆CH(CH₂)₃CHOMe]⁻, **1_d**. The reactivity of this class of ligands toward rhenium carbonyl complexes is reported and compared with that shown by the smaller congener cyclopentadienyl [C₅H₄CH₂CH(Me)OH]⁻, **5_a**, Cp^{OH}_a, and with the π-extended fluorenyl system [C₁₃H₈-CH₂CH(Me)OMe]⁻, **10_a**, Flu^{OMe}_a. The coordination of functionalized indenyl ligands shows a facile haptotropic behavior,⁹ and the reaction with Re(CO)₅Br allows the characterization of η¹-Ind_{a,d}^{OMe}Re(CO)₅ (**12_{a,d}**) and η³-Ind_{a,d}^{OMe}Re(CO)₄ (**13_{a,d}**) species. Steric requirements favor the monohapto species, whereas re-aromatization of the benzo-condensed ring is crucial in stabilizing the allylic coordination. DFT calculations support the experimental findings and clarify the lack of isolation of the η⁵ expected species. This goal is achieved only by reacting the solvento Re(CO)₃(NCMe)₂Br compound, although a strong asymmetrical π-coordination is observed in π-Ind_{b,c}^{OMe}Re(CO)₃ (**14_{b,c}**) complexes. Finally, the bulkiness of methyl or the electron-withdrawal phenyl 2-substituent is responsible for trapping the unstable alkoxide derivatives κ¹-O-Ind_{a,b}^ORe(CO)₅, **11_{a,b}**, reported as rare examples of the class of low-valent rhenium alkoxy species.

Results and Discussion

Ligand Preparation. In Chart 1 are collected the classes of novel five-electron donor ligands, which have been prepared

and tested in the reaction with rhenium carbonyl species of the type [Re(CO)_{5-n}(Solv)_nBr] (*n* = 0, 2; Solv = NCMe, THF). Only the main features of the selected ligands are reported in the discussion, while a full detailed account appears in the Experimental Section. As a general method, room-temperature addition of the appropriate oxide [CHR₁CHR₂]O (see Chart 1, path i) to a THF solution of sodium indenide¹⁰ promptly gives brick-red mixtures of the corresponding sodium salts [C₉H₆CHR₁CHR₂O]Na, **HInd_x^{ONa}**, **1_x**, which are characterized by their NMR data. In the case of propylene oxide, the ¹H single olefin resonance at δ 6.26 and for CHO methyne moiety at 4.30 ppm indicates the formation of sodium 1-(3*H*-inden-3-yl)propan-2-olate, [C₉H₆CH₂CH(Me)O]Na, **HInd_a^{ONa}**, **1_a**, as the unique anionic species. Modification of the reaction conditions such as thermal treatment, counterion, and solvent does not alter the regioselective attack, which is exclusively directed to the less impeded carbon atom in this case. Water quenching gives the corresponding alcohol C₉H₆[CH₂CH(Me)OH], **2_a** (Chart 1, path iv), which confirms the occurrence of a [H₁₋₃] prototropic shift. The heterocorrelated spectra assign the accidentally isochronous ¹³C NMR resonances found at δ 38.5 to the methylene group of the fused-Cp ring (3.45 ppm) and of the side chain (2.80 ppm), respectively.

It is known that counterion and solvent nature both drive the selectivity in the nucleophilic addition.⁸ Indeed, the reaction with lithium indenide in a THF-hexane (~85:15) solution, upon neutralization, gives rise to an analogous mixture of isomers, whose nature has been determined by ¹H NMR data. The H2 and H3 NMR multiplets,

(9) (a) Casey, C. P.; O'Connor, J. M. *Organometallics* **1985**, *4*, 384–388. (b) Casey, C. P.; Vos, T. E.; Brady, J. T.; Hayashi, R. K. *Organometallics* **2003**, *22*, 1183–1195.

(10) For selected patents see: (a) Hauck, F. P.; Reid, J.; Narayanan, V. L.; Cimarusti, C. M.; Haugwitz, R. D.; Sundenn, J. E. (E.R. Squibb & Sons, Inc.) Patent Appl. N. US1976000649116, 1977. (b) Hauck, F. P.; Sundenn, J. E.; Reid, J. (E.R. Squibb & Sons, Inc.) Patent Appl. N. US1977000820290, 1979. (c) Hauck, F. P.; Sundenn, J. E.; Reid, J. (E.R. Squibb & Sons, Inc.) Patent Appl. N. US1978000928483, 1979.

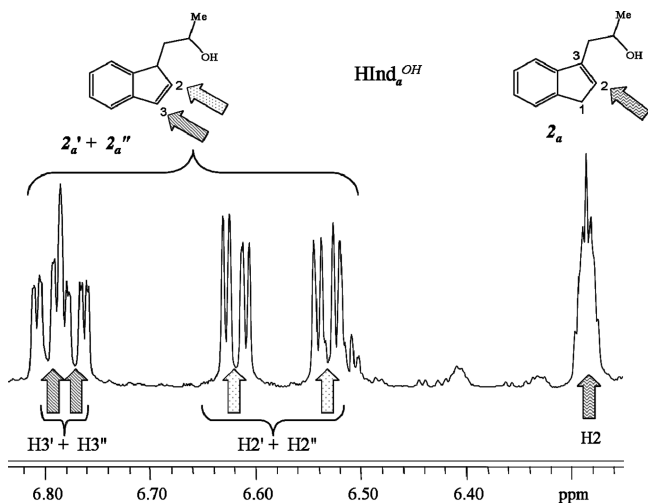


Figure 1. ^1H NMR spectra in CDCl_3 . Olefin region of the 2_a , $\text{HInd}_a^{\text{OH}}$, isomeric mixture.

upfield-shifted respectively in the ranges δ 6.52–6.64 and 6.76–6.82, indicate the prevalence of 1-substituted indenyl diastereomers (~66%) and a minor amount of 3-substituted 2_a (~33%) (see Figure 1).

The reaction with lithium fluorenyl (Chart 1, path iii) forms an almost equimolar mixture of lithium 1-(9*H*-fluoren-9-yl)propan-2-olate, $[\text{C}_{13}\text{H}_9\text{CH}_2\text{CH}(\text{Me})\text{O}]\text{Li}$ (6_a) and (lithium-9-fluorenyl)propan-2-ol, $[\text{C}_{13}\text{H}_8\text{CH}_2\text{CH}(\text{Me})\text{OH}]\text{Li}$ (7_a). The ^{13}C NMR upfield-shifted resonance at δ 40.6 is attributed to the tetrahedral C_9H moiety and ascertains the nature of 6_a , whereas the related signal at δ 134.6 is diagnostic for the alcoholic shiftamer 7_a . Water neutralization (Chart 1, path iv) gives yellow needles of 1-(9*H*-fluoren-9-yl)-propan-2-ol (8_a). Variable-temperature ^1H NMR experiments on the progressively dilute solutions of 8_a suggest H-bonding involvement, exhibiting a scarce temperature dependence for the hydroxy signal at δ 2.00. In the NOESY 1D experiments, the irradiation of the benzo-fused ring ortho-proton (H1, 7.57 ppm) causes a major enhancement in the methyne signal, whereas saturation of the corresponding benzo proton H8 (7.68 ppm) markedly affects the closest proton of the methylene (see A in Figure 2).

The reduced steric repulsions and the optimized hydroxyl hydrogen interactions both favor a flanked conformation (see Figure 2, structure A).¹¹ The minimum energy configuration in solution is retained in the solid state, as inferred by X-ray diffraction data (B) and also confirmed by DFT calculations *in vacuo* (C). An analogous synthesis of $\text{HFlu}_a^{\text{OH}}$, 8_a , has been run with the enantiopure *S*-propylene oxide, and the molecular structure of the latter, determined by X-ray crystal diffraction, is reported in Figure 3, while selected bond lengths and angles are listed in Table 1. The asymmetric unit of the orthorhombic cell contains two independent molecules with identical connectivities, an absolute *S* configuration at the quaternary asymmetric carbons [C(2) and C(22), respectively], and very similar bonding parameters. The H-atoms bonded to O-atoms in both independent molecules were located in the Fourier map. Extensive H-bonding exists within the crystal, since the OH group of each molecule acts at the same time as donor and

acceptor toward two different vicinal molecules. The three fused rings in the fluorene system are almost planar. As expected for these classes of compounds, the bonding parameters are in agreement with the different hybridizations of the C-atoms.

Conversely, lithium fluorenyl addition on the styrene oxide forms a nearly equimolar hydroxyl-anion mixture of Flu_b^{O} $[\text{C}_{13}\text{H}_9\text{CH}(\text{Ph})\text{CH}_2\text{OH}]^-$ (7_b) and the isomeric form Flu_c^{O} $[\text{C}_{13}\text{H}_9\text{CH}_2\text{CH}(\text{Ph})\text{OH}]^-$ (7_c). The withdrawing phenyl substituent quantitatively promotes proton O-migration (Chart 1, path iii), preventing the alcoholate isolation.

Like the indenide, the addition of NaCp as nucleophile yields regioselectively the shiftamer cyclopentadienylpropan-2-ol¹² $\text{Na}[\text{C}_5\text{H}_4\text{CH}_2\text{CH}(\text{Me})\text{OH}]$, $\text{NaCp}_a^{\text{OH}}$, 5_a (Chart 1, path ii). The ^1H NMR spectra of the anion show a single hydroxy group at δ 2.2 and a downfield-shifted resonance at δ 3.7 for the methyne moiety, ruling out the occurrence of 1-cyclopenta-1,4-dienylpropan-2-ol,⁸ formed by the alternative epoxide ring-opening. No appreciable dimerization has been detected in the substituted cyclopentadiene HCp^{OH} tetrahydrofuran solution, although it has been found to occur in similar polar solvents.^{7d} Understandably, the selective O-alkylation of 1_{a-d} (Chart 1, path v) is largely critical, since it depends on the counterion nature, solvent polarity, and microenvironment heterogeneity of the alkylating mixture.¹³ It is worth mentioning that the addition of methyl iodide in low-polar solvents partially gives ring alkylation (30–40%). This supports our choice of using methyl triflate instead. However, a sequenced deprotonation/alkylation tandem reaction is required to transform quantitatively the alcoholic forms (Ind_x^{OH} , 2_x ($x = a-d$), and Flu_a^{OH} , 8_a) to the corresponding ether derivatives ($\text{Ind}_x^{\text{OMe}}$, 3_x , and $\text{Flu}_a^{\text{OMe}}$, 9_a). Finally, deprotonation of type 3_x ($x = a-d$) and 9_a affords the anionic derivatives 4_x ($x = a-d$) and 10_a , which are readily suitable for rhenium coordination.

Coordination Chemistry. Treatment of alcoholates $\text{HInd}_x^{\text{ONa}}$, 1_x ($x = a, b$), with $\text{Re}(\text{CO})_5\text{Br}$ forms the corresponding alkoxy species of the type $\kappa^1\text{O-HInd}_x^{\text{O}}\text{Re}(\text{CO})_5$, 11_x , which were isolated as powdered solids and characterized without any further purification, in order to prevent the decomposition observed during the chromatography (on alumina, silica, or Celite gel). No remarkably shifted NMR signals of the adduct, with respect to the alcoholate $1_{a,b}$, suggests a strongly polarized $\text{Re}^{(1)}-\text{O}$ bond. The nonstabilizing effect of the metal–oxygen lone pair interaction¹⁴ is responsible for the scarcity of monomeric rhenium low-valent carbonyl species. Metal coordination affects mainly the CHO methyne NMR signals, which appear remarkably deshielded at δ ^1H 4.06 and ^{13}C 66.9 ppm in the case of 11_a . DFT calculations and subsequent Mulliken analysis on the latter confirm the large charge separation between the O-alcoholate (−0.74) moiety and the $\text{Re}(\text{I})$ (+0.80) atoms (Figure 4).

The occurrence of four distinct IR absorptions (ν , KBr 2021 m, 1914 s, 1903 s, 1895 s) is due to restricted rotation of the tether chiral O-pendant.¹³ $\text{Re}(\text{CO})_5$ fragment dimerization and trihydride¹⁵ $\text{Re}_3(\mu\text{-H})_3(\text{CO})_{12}$ or hydroxyl

(11) Price, C. J.; Zeits, P. D.; Reibenspies, J. H.; Miller, S. A. *Organometallics* **2008**, *27*, 3722–3727.

(12) Tantillo, D. J.; Hoffmann, R. *Acc. Chem. Res.* **2006**, *39*, 477–486.

(13) Oltmanns, M.; Mews, R. *Z. Naturforsch.* **1980**, *35b*, 1324.

(14) Turova, N. Y.; Turevskaya, E. P.; Kessler, V. G.; Yanovskaya, M. I. *The Chemistry of Metal Alkoxydes*; Kluwer: Dordrecht, 2002.

(15) (a) Andrews, M. A.; Kirtley, S. W.; Kaesz, H. D.; Cooper, C. B. *Inorg. Synth.* **1977**, *17*, 66. (b) Ciani, G.; Sironi, A.; D'Alfonso, G.; Romiti, P.; Freni, M. *J. Organomet. Chem.* **1983**, *254*, C37.

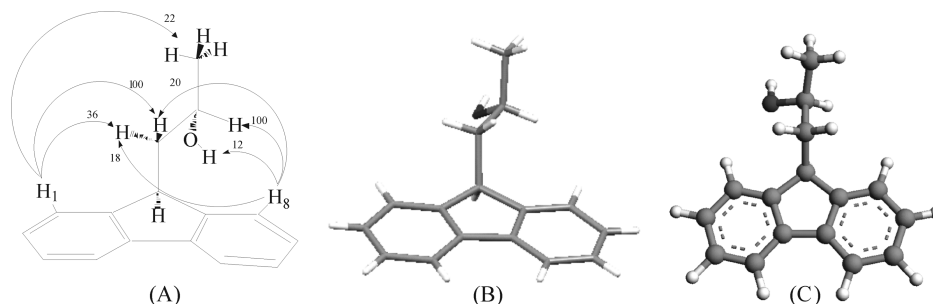


Figure 2. $\text{HFlu}_a^{\text{OH}}$, $\mathbf{8}_a$ structures: (A) 1D ^1H NOESY interactions in CDCl_3 . The numbers over the arrows indicate the percentage increase of the signal relative to the saturation of H_1 and H_8 . (B) X-ray structure. (C) DFT calculations.

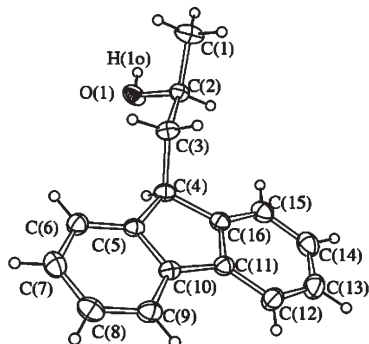


Figure 3. Molecular structure of $\text{HFlu}_a^{\text{OH}}$, $\mathbf{8}_a$. Thermal ellipsoids are drawn at the 30% probability level. Only one of the two independent molecules present within the asymmetric unit is represented. [O(1)–H(1o) 0.836(19) Å; H(1o)···O(2)#1 2.02(2) Å; O(1)···O(2)#1 2.837(2) Å; O(1)–H(1o)–O(2)#1 166(4)° for the first independent molecule acting as a donor; O(2)–H(2o) 0.84(2) Å; H(2o)···O(1)#2 1.90(2) Å; O(2)···O(1)#2 2.721(2) Å; O(2)–H(2o)–O(1)#2 166(4)° for the second independent molecule]. Mean deviations from the least-squares planes are 0.0475 and 0.0561 Å for the two independent molecules, respectively.

tetrahrenium^{9a} $[\text{Re}(\text{CO})_3\text{OH}]_4$ formation are observed as common degradation paths.

The reaction of ether indenide $[\text{C}_9\text{H}_6\text{CH}(\text{R}_1)\text{CH}(\text{R}_2)\text{OMe}]\text{Li}$ [$\text{R}_1 = \text{H}$, $\text{R}_2 = \text{Me}$; $\text{R}_1 = \text{R}_2 = -(\text{CH}_2)_3-$], $\mathbf{4}_x$ ($x = a, d$), derivatives with $\text{Re}(\text{CO})_5\text{Br}$ promptly yields a nearly equimolar mixture of η^1 - $[\text{C}_9\text{H}_6(\text{CH}_2\text{CH}(\text{Me})\text{OMe})\text{Re}(\text{CO})_5]$, $\mathbf{12}_a$, and η^3 - $[\text{C}_9\text{H}_6(\text{CH}_2\text{CH}(\text{Me})\text{OMe})\text{Re}(\text{CO})_4]$, $\mathbf{13}_a$ (Scheme 1), which are characterized by their NMR data, after separation by column chromatography.

As observed for analogous systems,¹⁷ the downfield-shifted NMR signals (^{13}C δ 142.7 and ^1H δ 8.4), attributed to the olefin C2H moiety, strongly support that the first eluted band is the allylic-coordinated¹⁸ η^3 - $[\text{C}_9\text{H}_6\text{CH}_2\text{CH}(\text{Me})\text{OMe}]\text{Re}(\text{CO})_4$, $\mathbf{13}_a$, species. Conversely, the shielded

Table 1. Crystal Data and Experimental Details for $\text{HFlu}_a^{\text{OH}}$, $\mathbf{8}_a$

formula	$\text{C}_{16}\text{H}_{16}\text{O}$
fw	224.29
T , K	291(2)
λ , Å	0.71073
cryst syst	orthorhombic
space group	$\text{Pna}2_1$
a , Å	1.9507(7)
b , Å	11.9175(10)
c , Å	26.323(2)
cell volume, Å ³	2494.2(4)
Z	8
D_c , g cm ⁻³	1.195
μ , mm ⁻¹	0.073
$F(000)$	960
cryst size, mm	0.31 × 0.18 × 0.16
θ limits, deg	1.55–27.99
index ranges	–10 ≤ h ≤ 10 –15 ≤ k ≤ 15 –34 ≤ l ≤ 34
reflns collected	26 611
indep reflns	3055 [$R_{\text{int}} = 0.0271$]
completeness to θ_{max}	99.3%
data/restraints/params	3055/3/315
goodness on fit on F^2	1.106
R_1 ($I > 2\sigma(I)$)	0.0462
wR_2 (all data)	0.1235
largest diff peak and hole, e Å ⁻³	0.323/–0.374

^{13}C NMR resonance (δ 38.5) exhibited by the second fraction is diagnostic for the aliphatic character¹⁹ of the C_1H –Re moiety in η^1 - $[\text{C}_9\text{H}_6\text{CH}_2\text{CH}(\text{Me})\text{OMe}]\text{Re}(\text{CO})_5$, $\mathbf{12}_a$. At room temperature, the haptomers $\mathbf{12}_x$ ($x = a, d$) convert quantitatively to $\mathbf{13}_x$ ($x = a, d$) in polar solvents (CH_2Cl_2 , MeCN). Differently from the similar η^1 - $[\text{C}_9\text{H}_6(\text{C}_6\text{F}_5)]\text{Re}(\text{CO})_5$,²⁰ distinct carbonyl patterns have been observed in both the ^{13}C NMR and IR spectra. This inequivalence is caused by the hindered rotation of the chiral side arm, whose presence precludes H_{1-3} migration.¹⁹ No isolation of η^5 -coordinated species, but only degradation²¹ to $[\text{Re}_2(\mu\text{-OMe})_3(\text{CO})_6]^-$ or $[\text{Re}_2(\mu\text{-OH})_3(\text{CO})_6]^-$ is detected by thermal treatment of $\mathbf{12}_x$ or $\mathbf{13}_x$ (at room temperature and at refluxing THF). This observation prompted us to study the free energy profile by DFT calculations, which reveal a very small stability for the η^5 -haptomer $\mathbf{14}_a$, compared to the kinetic mono-hapto species $\mathbf{12}_a$ (Figure 5). Such a limited

(16) Pannarello, A. P.; Vassilyev, O.; Khinast, J. G. *Synlett* **2005**, 5, 797–800.

(17) (a) Trost, B. H.; Vidal, B.; Thommen, M. *Chem.—Eur. J.* **1999**, 5, 1055. (b) Stoll, M. E.; Belanzoni, P.; Calhorda, M. J.; Drew, M. G. B.; Felix, V.; Geiger, W. E.; Gamelas, C. A.; Goncalves, I. S.; Romao, C. C.; Veiros, L. F. *J. Am. Chem. Soc.* **2001**, 123, 10595, and references therein.

(18) (a) Brisdon, B. J.; Edwards, D. A.; White, J. W. *J. Organomet. Chem.* **1979**, 175, 113. (b) Aechter, B.; Polborn, K.; Beck, W. *Z. Anorg. Allg. Chem.* **2001**, 627, 43. (c) Beattie, I. R.; Emsley, J. W.; Lindon, J. C.; Sabine, R. M. *J. Chem. Soc., Dalton Trans.* **1975**, 1264. (d) Lippmann, E.; Robl, C.; Berke, H.; Kaesz, H. D.; Beck, W. *Chem. Ber.* **1993**, 126, 933. (e) Moll, M.; Behrens, H.; Seibold, H. J.; Merbac, P. *J. Organomet. Chem.* **1983**, 248 329. (f) Ascenso, J. R.; Goncalves, I. S.; Herdtweck, E.; Romão, C. C. *J. Organomet. Chem.* **1996**, 508, 169.

(19) Herrmann, W. A.; Kuhn, F. E.; Romao, C. C. *J. Organomet. Chem.* **1995**, 489, C56.

(20) Deck, P. A.; Fronczek, F. R. *Organometallics* **2000**, 19, 327.
(21) (a) Roger, A.; Egli, A.; Ulrich, A.; Hegetschweiler, K.; Gramlich, V.; Schubiger, P. A. *J. Chem. Soc., Dalton Trans.* **1994**, 19, 2815. (b) Jiang, C. H.; Wen, Y. S.; Liu, L.-K.; Hor, T. S. A.; Yan, Y. K. *Organometallics* **1998**, 17, 173. (c) Jiang, C.; Hor, T. S. A.; Yan, Y. K.; Henderson, W.; McCaffrey, L. J. *J. Chem. Soc., Dalton Trans.* **2000**, 3197–3203.

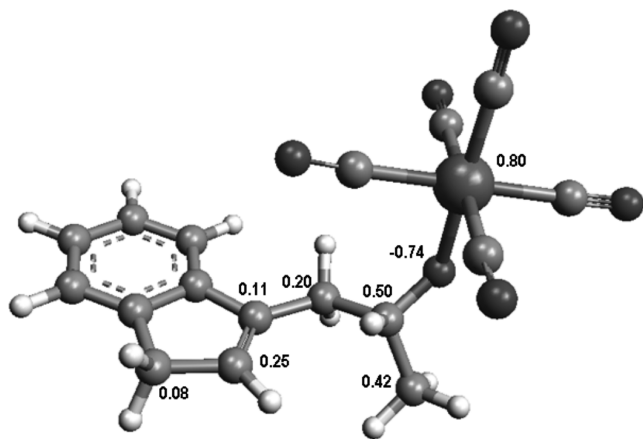


Figure 4. DFT calculations on the rhenium alkoxide **11_a**. Only relevant Mulliken charges have been indicated.

stability is the plausible reason for the lack of its isolation, as the degradation products are thermodynamically favored. According to Calhorda and Veiros's pioneering work,²² the Re–C bond lengths, indicating two short bonds [2.472 (C₂), 2.439 (C₃) Å] and a much longer one [3.160 (C₁) Å], together with the ¹³C NMR upfield-shifted ring junction signals, falling at δ 138.1, 138.8, both indicate [$\eta^2 + \eta^1$] as a better description for the allylic-coordinated **13_a**.

The reaction with cyclopentylmethoxy indenide [$C_9H_6-CH(CH_2)_3CHOMe$]Li, **LiInd_d^{OMe}**, **4_d**, analogously yields a mixture of η^3 -Ind_d^{OMe}Re(CO)₄ (**13_d**) and the σ -coordinated (**12_d**) haptomers. The highly deshielded NMR signals,^{17b} found at δ 142.3 (¹³C) and 8.5 (¹H) for the C2H moiety and at δ 146.4 and 145.2 for the junction carbon atoms, ascertain the nature of **13_d**. The four distinct IR carbonyl absorptions of **12_d** (ν , KBr 2088 w, 2037 m, 1996 vs, 1893 m) and its upfield-shifted ¹H NMR triplet (δ ¹H 2.83), attributed to the σ -bound CH(Re) group, support its structure as η^1 -[C₉H₆CH(CH₂)₃CHOMe]Re(CO)₅.

The isolation of η^5 -coordinated species has been accomplished only by reacting the phenyl-substituted ether indenides [C₉H₆CH(R₁)CH(R₂)OMe]Li [R₁ = H, R₂ = Ph; R₁ = Ph, R₂ = H], **4_x** ($x = b, c$), with the labile Re(CO)₃(NCMe)₂Br,²³ yielding the desired **14_{b,c}** complexes, which have been characterized by their spectroscopic features. In particular, η^5 -[C₉H₆CH₂CH(Ph)OMe]Re(CO)₃, **14_b**, has been assigned by the peculiar C3 (δ 83.8) and C2 (δ 120.0) ¹³C NMR signals. The marked downfield shift for the latter is likely due to the combined effect²⁴ of the substitution and the electron charge distribution.²⁵

The DFT-calculated Re–C distances of the complex **14_b** [η^2 : 2.555 (C₄); 2.561 (C₅) + η^3 : 2.412 (C₂); 2.420 (C₃) + 2.456

(C₁) Å] (see Figure 6) indicate an asymmetric charge distribution. Upon standing at –20 °C in acetonitrile solution, the latter gives the solvento η^5 -Ind_b^{OMe}Re(CO)₂(NCMe), **15_b**, showing a similar bond description of the type $\eta^2 + (\eta^2 + \eta^1)$, as inferred by DFT calculation [Re–C bond lengths (Å): 2.590 (C₅); 2.551 (C₄) + 2.415 (C₂); 2.374 (C₃) + 2.487 (C₁)]. The IR ligand absorptions at lower frequencies (ν 2224 w, CN; 2035 m, 1937 m, CO) and the NMR signals relative to the bound MeCN (IR; ¹H δ 5.1 MeCN, ¹³C 121.3; MeCN) both support the nature of species **15_b**, which in turn gives a reddish precipitate at room temperature upon addition of chlorinated solvent. The nature of the resulting $\kappa^1O:\eta^5$ -Ind_b^{OMe}Re(CO)₂, **16_b** (see Scheme 2), has been assigned by the upfield-shifted ¹H NMR signal at δ 1.19 for the bound methoxy moiety. After dissolution in acetonitrile, the chelate species **16_b** reproduces the solvento species **15_b**.

Furthermore, assuming that more accessible space around the metal site may favor intermediate interception, we investigated the pendant chelate coordination of the less congested η^5 -Ind_c^{OMe}Re(CO)₃, **14_c**, bearing the side-arm phenyl substituent in the 1-position (see Scheme 3). Unfortunately, in acetonitrile, degradation prevails. However, by using a milder coordinating solvent such as THF, prompt decarbonylation occurs by forming η^5 -Ind_c^{OMe}Re(CO)₂(THF), **15_c**.

The ¹H NMR spectrum of Ind_c^{OMe}Re(CO)₂(THF), **15_b**, showing the NMR resonances at δ 4.25 and 3.36 for H2 and H3, respectively, indicates a stronger electron density perturbation due to 1-phenyl effects (δ CHPh 4.12, see Scheme 3), compared with the 2-phenyl MeCN-adduct **15_b** (¹H NMR δ 4.2 H2; 4.4 H3). In addition DFT calculations evidence the skewed ($\eta^2 + \eta^3$) bonding description [Re–C bond distances (Å): 2.560 (C₅); 2.573 (C₄) + 2.360 (C₂); 2.375 (C₃); 2.359 (C₁)]. The presence of broad signals at δ 1.73 and 3.58, attributed to the ligated THF, validates the proposed structure. Dichloromethane addition promotes THF displacement by methoxy assistance, causing precipitation of the red $\kappa^1O:\eta^5$ -Ind_c^{OMe}Re(CO)₂, **16_c**. The ¹³C NMR ring junction signals (δ 144.6, 147.4) exhibit low-shifted values, indicating electron density perturbation. Accordingly with the calculated Re–OMe interaction (2.424 Å), the presence of a chelate structure is also supported by the upfield-shifted NMR resonances (¹H δ 1.11; ¹³C δ 22.7) of the metal-bound methoxy function.¹⁹ However, dissolution of complex **16_c** by donor media promptly causes chelate release, which confirms its hemilabile nature (Scheme 3).

No allylic solvento intermediates but only pentahapto derivatives could be intercepted by monitoring the formation of the chelate $\kappa^1O:\eta^5$ -Ind_{b,c}^{OMe}Re(CO)₂, **16_{b,c}**, likely due to the low basicity of THF, MeCN, or the side-arm methoxy ligand, according to Basolo's kinetic investigations²⁶ on the S_N2 substitution of IndMn(CO)₃ by basic phosphines. The calculated more stable conformer of **14_c** maximizes the nonbonding electronic interactions between the carbonyl ligands and the alkyl chain (methoxy, CO···H–CH₂O, 3.24 Å, and methylene, CO···H–CH, 3.31 Å), reducing at the same time the steric repulsions.

The higher stability (~13 kcal mol⁻¹), shown by the MeCN intermediate η^5 -Ind_{b,c}^{OMe}Re(CO)₂(MeCN), **15_b**, with respect to the analogous THF derivative **15_c** is in agreement with the symbiotic soft–soft interaction between

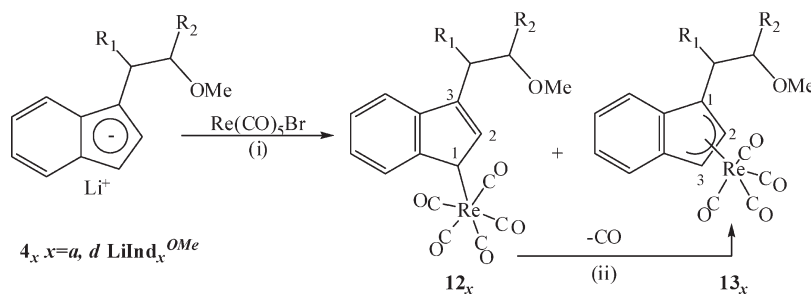
(22) (a) Veiros, L. F. *Organometallics* **2000**, *19*, 3127–3136. (b) Calhorda, M. J.; Gamelas, C. A.; Romão, C. C.; Veiros, L. F. *Eur. J. Inorg. Chem.* **2000**, 331–320. (c) Veiros, L. F. *Organometallics* **2006**, *25*, 2266–2273. (d) Bradley, C. A.; Lobkovsky, E.; Chirik, P. J. *J. Am. Chem. Soc.* **2003**, *125*, 8110–8111. (e) Bradley, C. A.; Lobkovsky, E.; Keresztes, I.; Chirik, P. J. *J. Am. Chem. Soc.* **2005**, *127*, 10291–10304. (f) Veiros, L. F. *Organometallics* **2006**, *25*, 4698–4701.

(23) Faroni, M. F.; Kraus, K. F. *Inorg. Chem.* **1970**, *9*, 1700.

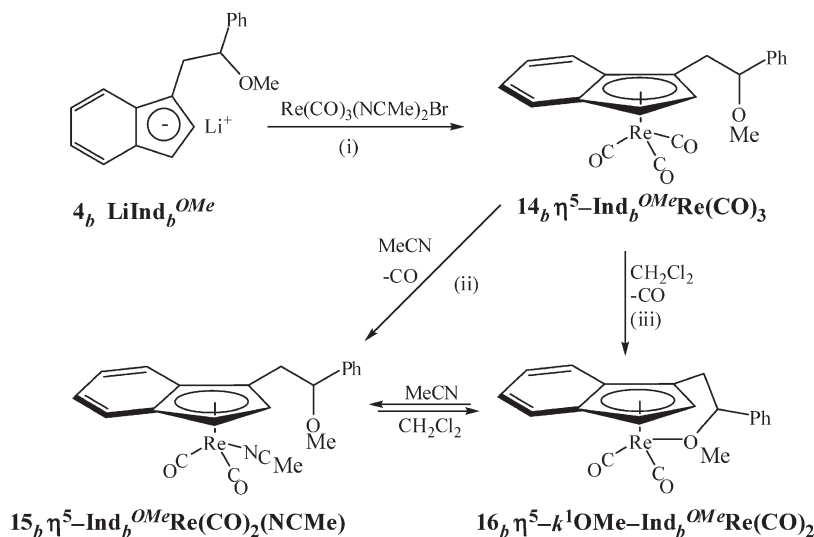
(24) Ascenso, J. R.; Gonçalves, I. S.; Herdtweck, E.; Romão, C. C. *J. Organomet. Chem.* **1996**, *508*, 169.

(25) (a) Marder, T. D.; Calabrese, J. C.; Roe, D. C.; Tulip, T. H. *Organometallics* **1987**, *6*, 2012. (b) Calhorda, M. J.; Felix, V.; Veiros, L. F. *Coord. Chem. Rev.* **2002**, *230*, 49. (c) Calhorda, M. J.; Veiros, L. F. *Coord. Chem. Rev.* **1999**, *185–186*, 37–51.

(26) Ji, L.-N.; Rerek, M. E.; Basolo, F. *Organometallics* **1984**, *3*, 740–745.

Scheme 1^a

^a $R_1 = H$, $R_2 = Me$; $d R_1 = R_2 = CH(CH_2)_3CH$. Reaction conditions: (i) THF, $-78\text{ }^\circ\text{C}$ to rt; (ii) CH_2Cl_2 or MeCN, rt, 24 h.

Scheme 2. Synthesis and Haptotropic Rearrangement of Ind_b^{OMe} Re-Coordinated Species^a

^a Reaction conditions: (i) THF, $-78\text{ }^\circ\text{C}$, 2 h; (ii) $-20\text{ }^\circ\text{C}$, 12 h; (iii) rt, 16 h.

Re(I) and $NA\equiv CMe$, predicted by the hard–soft acid–base (HSAB) theory and supported by the calculated frontier orbitals. Indeed, acetonitrile participates as a σ -donor as well as a π -acceptor in the bonding description and globally contributes to lowering the energetics of the MeCN with respect to the THF intermediate complexes (see DFT frontier orbitals for **15_{b,c}**, Figure S4, S5). Finally, in spite of the comparable Re–O enthalpic contribution and the favorable entropic factor, the metallacycle strain is likely to be responsible for the instability of the resulting chelate $\kappa^1O:\eta^5\text{-Ind}_{b,c}^{OMe}Re(CO)_2$, **16_{b,c}**. As alternative synthetic route,²⁷ photochemical reaction of $Re(CO)_5Br$ with the neutral $C_9H_7CH_2CH(Me)OH$, **2_a**, leads to the exclusive isolation of the tetrahydroxy $Re_4(CO)_{12}(OH)_4$ compound.^{9a}

Analogous reactions of the smaller $[C_5H_4CH_2CH(Me)OH]Na$, Cp_a^{OH} , **5_a**, and of the larger $[C_{13}H_8CH_2CH(Me)OH]Li$, $LiFlu_a^{OMe}$, **10_a**, five-electron-donor congeners permit a comparative study with the above-described Ind_a^{OMe} , **4_a**. In the reaction of **5_a** with $Re(CO)_5Br$, degradation to $[Re_2(\mu-OH)_3(CO)_6]^-$ prevails, although DFT calculations indicate a lower energy ($\sim -15\text{ kcal mol}^{-1}$) for the pentahapto $Cp_a^{OH}Re(CO)_5$ species (Figure 8). However, from the solvent derivative $Re(CO)_3(THF)_2Br$ it has been possible

to isolate the title $\eta^5\text{-Cp}^{OH}Re(CO)_3$, **17_a**. Chiral side-arm-impeded rotation on the NMR time scale is detected by the distinct ^{13}C ring resonances at δ 84.5, 84.6, 84.9, 85.3, and 107.4. Such inequivalence, which is commonly observed in the much more hindered π -systems,²⁸ is ascribed to hydroxyl interactions, since the 1H NMR OH signal at δ 4.05 appears markedly downfield-shifted, compared to the corresponding signal (δ 2.03) of the neutral HCP^{OH} species. Analogously $LiFlu_a^{OMe}$, **10_a**, gives a purple solution, showing a five-absorption IR pattern (2078w, 2031w, 1995s, 1977vs, and 1953m cm^{-1}). The ESI⁺ mass data [m/z , %: 571 $[M + H]^+$ (25), 515 $[M - 2CO]^+$ (100)] and the ^{13}C NMR signal at δ 83.4, indicating the presence of the σ -coordinated Re–C₉ moiety, are consistent with the formulation of the metathesis adduct²⁹ $\eta^1\text{-Flu}_a^{OMe}Re(CO)_5$, **18_a**. Thermolytic decarbonylation does not promote the formation of the expected penta-hapto derivative, as reported by other authors,³⁰ but only degradation to $[Re_2(\mu-OMe)_3(CO)_6]^-$. In light of the experimental path, DFT calculations on the fluorenyl complexes' energetics (Figure 8) show that the monohapto coordinating mode is the

(28) Le Bideau, F.; Henique, J.; Pigeon, P.; Joerger, J. M.; Top, S.; Jaouen, G. *J. Organomet. Chem.* **2003**, 668, 140.

(29) Drago, D.; Pregosin, P. S.; Razavi, A. *Organometallics* **2000**, 19, 1802.

(30) (a) Young, K. M.; Miller, T. M.; Wrighton, M. S. *J. Am. Chem. Soc.* **1990**, 112, 1529–1537. (b) Mejdrich, A. L.; Hanks, T. W. *Synth. React. Inorg. Met. – Org. Chem.* **1998**, 28, 953–973.

(27) (a) Zhou, Y.; Dewey, M. A.; Gladysz, J. A. *Organometallics* **1993**, 12, 3918. (b) Miguel, D.; Steffan, U.; Stone, F. G. A. *Polyhedron* **1988**, 7, 443. (c) Khayatpoor, R.; Shapley, J. R. *Organometallics* **2000**, 19, 2382.

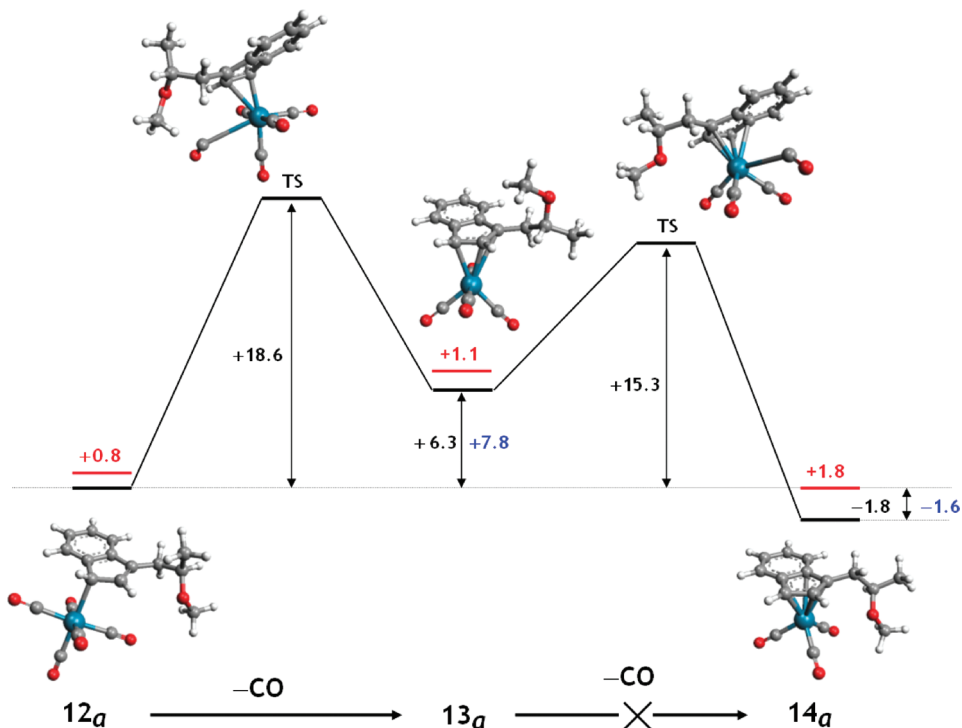


Figure 5. DFT-optimized structures for compounds **12_a**, **13_a**, and **14_a** and free energy profile (kcal mol⁻¹). In red is reported the relative energy of the less stable conformer. Alterations of the calculated free energies upon the inclusion of solvent effects (MeCN, $\epsilon = 37.5$) are shown in blue.

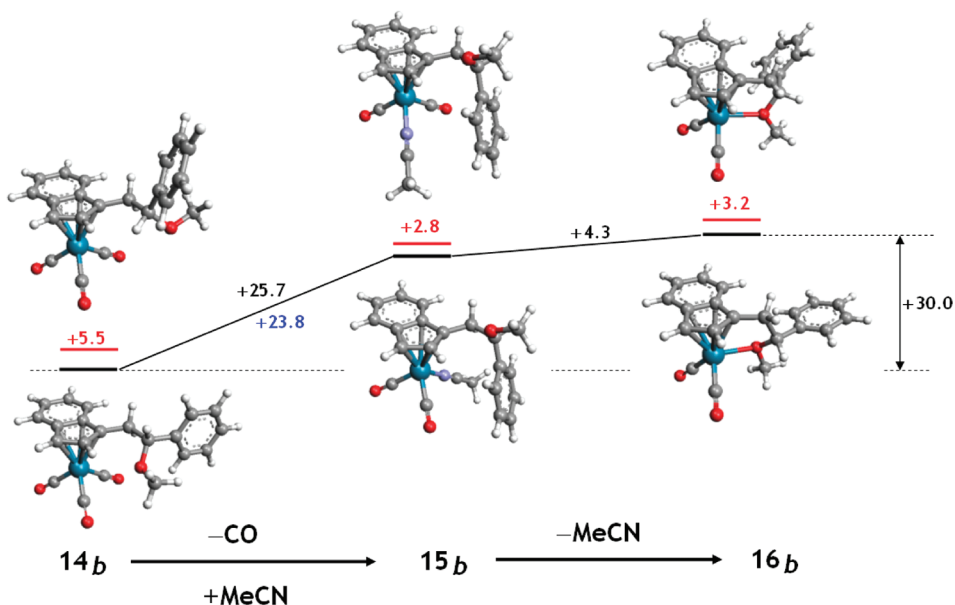


Figure 6. DFT-optimized structures and free energy calculations (kcal mol⁻¹) of the lowest and the highest conformations for η^5 -Ind_b^{OMe}Re(CO)₃, **14_b**; η^5 -Ind_c^{OMe}Re(CO)₂(MeCN), **15_b**; and $\kappa^1\text{O}:\eta^5$ -Ind_b^{OMe}Re(CO)₂, **16_b**, species. The relative energy of the less stable conformer is reported in red. The effect of the inclusion of the solvent (MeCN, $\epsilon = 37.5$) on the free energy is shown in blue.

preferred one, allowing the benzo-condensed rings to retain their aromatic character.

Conclusions

This report constitutes a contribution to the synthesis of the new O-functionalized indenyl (**Ind^O**), cyclopentadienyl (**Cp^O**), and fluorenyl (**Flu^O**) ligands and to the chemistry of their rhenium carbonyl complexes. In the case of **4_a**,

[C₉H₅CH₂CH(Me)OMe]Li, **Ind_a^{OMe}**, the reaction with Re(CO)₅Br permits isolation and characterization of both the monohapto- and trihapto-Re carbonyl species. However, the expected transformation to η^5 -coordinated species has never been observed, even under thermal treatment, leading instead to degradation products. The DFT free energy profile confirms that the penthapto coordination is essentially isoenergetic with respect to the monohapto one, with the entropic contributions playing a crucial role. Only by using

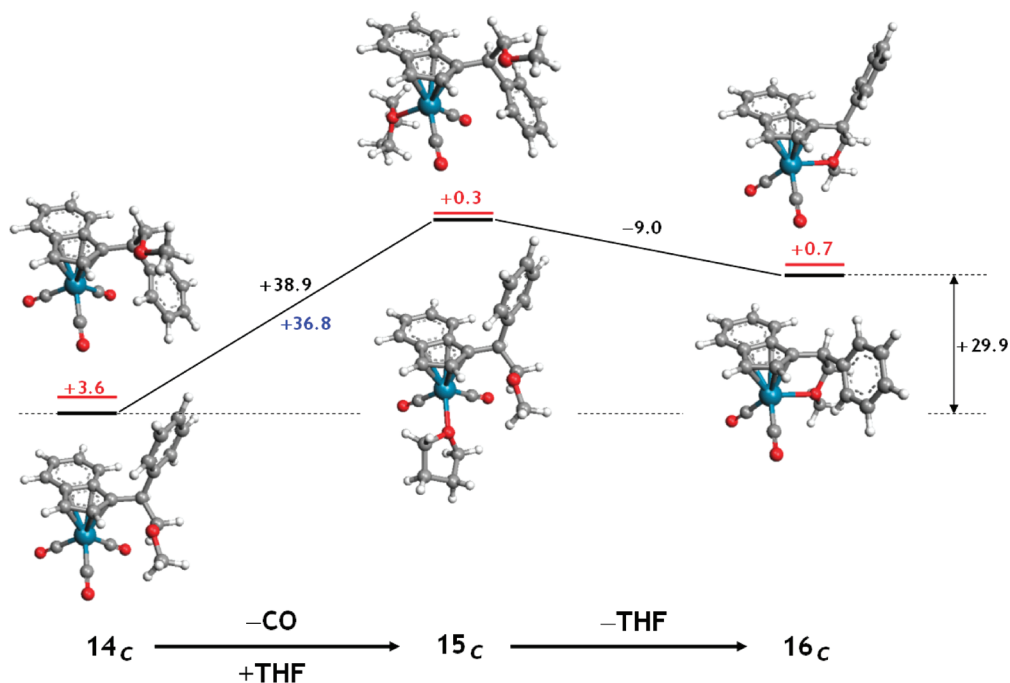


Figure 7. DFT-optimized structures and free energy calculations (kcal mol^{-1}) of the lowest and the highest conformations for η^5 - $\text{Ind}_c^{\text{OMe}}\text{Re}(\text{CO})_3$, **14_c**; η^5 - $\text{Ind}_c^{\text{OMe}}\text{Re}(\text{CO})_2(\text{THF})$, **15_c**; and $\kappa^1\text{O}:\eta^5$ - $\text{Ind}_c^{\text{OMe}}\text{Re}(\text{CO})_2$, **16_c**, structures. The relative energy of the less stable conformer is reported in red. The effect of the inclusion of the solvent (THF, $\epsilon = 7.58$) on the free energy is shown in blue. The η^5 -coordination in **15_c** is better described as the sum of the distinct hapticities ($\eta^2 + \eta^3$).

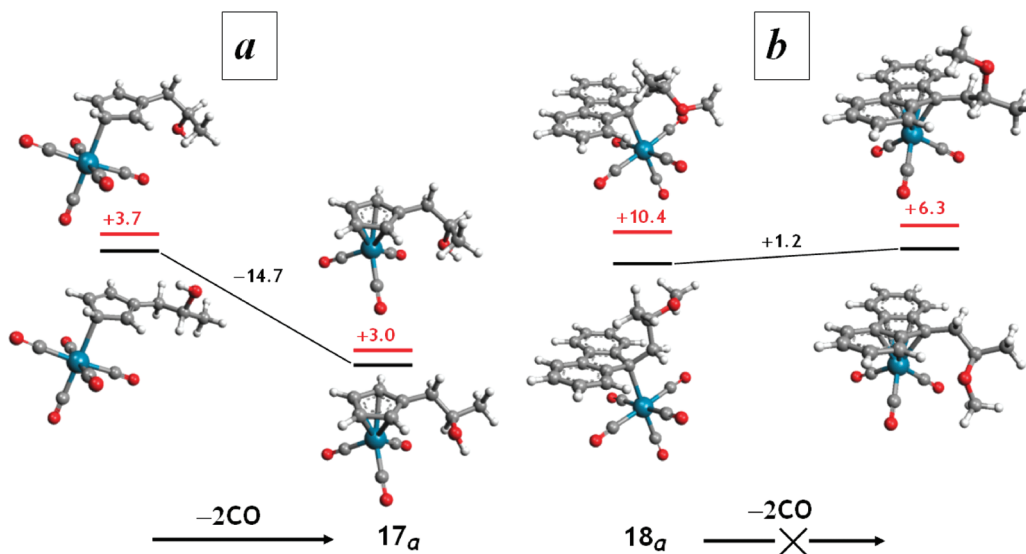
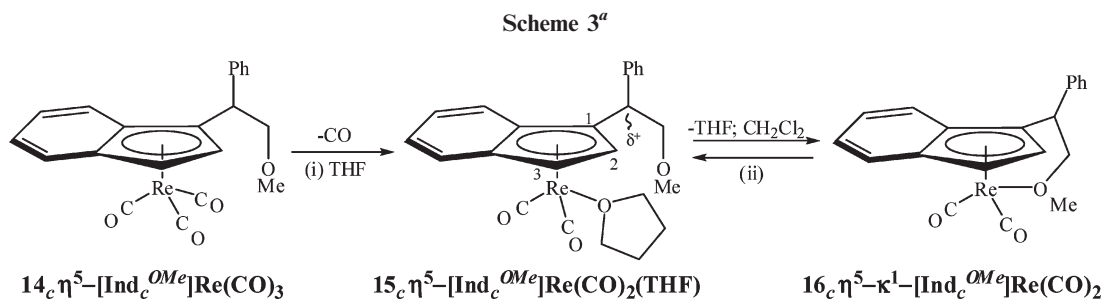


Figure 8. DFT-optimized structures and free energy calculations (kcal mol^{-1}) of the lowest and the highest conformations for haptomers of the type (a) η^5 - $\text{Cp}_a^{\text{OH}}\text{Re}(\text{CO})_5$, **17_a**, and (b) η^1 - $\text{Flu}^{\text{OMe}}\text{Re}(\text{CO})_5$, **18_a**, and the corresponding η^1 and η^5 unobserved parent structures. The relative energy of the less stable conformer is shown in red.



^a Reaction condition: (i) THF, -20°C , 6 h; (ii) THF, rt, 6 h.

Re(CO)₃(Solv)₂Br (Solv = MeCN, THF) as precursor does the interception of π -coordinated solvento η^5 -Ind_{b,c}^{OMe}Re(CO)₂(Solv) (Solv = MeCN, THF), **15**_{b,c}, species and of the chelate η^5 -Ind_{b,c}^{OMe}Re(CO)₂, **16**_{b,c}, become possible. This takes place by promotion of a large excess of the solvent as reactant, in spite of the unfavorable energies predicted by DFT calculations. The introduction of the solvent effects into the DFT theoretical approach, through a simple continuum dielectric model, always plays only a marginal role and does not change significantly the free energy profiles. Another effect that has been fully evidenced is the relevant bonding asymmetry shown by the tri- and penta-hapto complexes, which in all cases are better described as ($\eta^2 + \eta^1$) or ($\eta^2 + \eta^3$), respectively. The tuning of the ligand stereoelectronic requirements and the nature of the solvent both play a relevant role in choosing the preferred hapticity. The donor side arm, such as methyl or cyclopentyl substituents, promote η^1 - and η^3 -coordinating modes as **12**_{a,d} and **13**_{a,d}, whereas the phenyl electron-withdrawing effect causes the stabilization of the pentahapto derivatives **14**_{b,c}, **15**_{b,c}, and **16**_{b,c}. As important features, the carbonyl substitution by the π -extended O-functionalized cycloolefin (Ind^O and Flu^O) is sensitive to both size and basicity of the pendant chain substituents and to the solvent nature. Therefore, the introduction of an O-side arm seems to alter dramatically the stability of the resulting Cp-like rhenium species. The calculations confirm relevant shift of the electron density in all the η^5 -coordinating modes. The reduced hapticities observed in the indenyl and fluorenyl rhenium carbonyl derivatives favor (a) the re-aromatization of the benzo-condensed ring(s) in both π -extended polyenes, (b) a smaller hindrance for the side-arm rotation, by reduction of steric repulsion, and (c) the maximization of nonbonding interactions between carbonyl ligands and alkyl-chain moieties in the preferably adopted conformations.

Computational Details

Ab initio DFT calculations have been performed by using the ADF 2007.01 quantum chemistry package and through the built-in TZP basis and the BLYP functional.^{31a,31b} Inner orbitals (1s for carbon and oxygen and 1s, 2s, 2p, 3s, 3p, 3d, 4s, 4p, and 4d for rhenium atom) have been kept frozen; this corresponds to the “small core” option in the definition of the basis set for the ADF code. Geometry optimizations, without symmetry constraints, were carried out in Cartesian coordinates using default convergence criteria (10⁻³ au for energies and 10⁻² au Å⁻¹ for gradients). Free energy calculations have been performed using standard statistical mechanics formulas,^{31c} starting from the calculated harmonic frequencies and assuming ideal gas behavior. Free energy variations correspond to differences of the free energies *in vacuo* of the shown structures, increased or diminished by the free energies of the exiting (−X, X = CO, MeCN, THF) or entering (+X, X = MeCN, THF) species, respectively. Solvent effects for **12**_a, **13**_{a,b,c}, **14**_{a,b,c}, and **15**_{b,c} species have been taken into account according to the COSMO^{31d} solvation model. The package has been implemented in ADF 2007.1, by using for MeCN $\epsilon = 37.5$ as dielectric constant and 2.76 Å as solvent radius, or $\epsilon = 7.58$ as dielectric constant and a solvent radius of 3.18 Å for THF.

Experimental Section

All manipulations were carried out under an argon atmosphere and by using standard Schlenk techniques. Anhydrous solvents were dried and distilled under nitrogen prior to use and saturated with nitrogen.³³ Glassware was heated under vacuum prior to use. The prepared derivatives were characterized by elemental analysis and spectroscopic methods. The IR spectra were recorded with a Perkin-Elmer Spectrum 2000 FT-IR spectrometer. The routine NMR spectra (¹H, ¹³C, DEPT) were recorded using a Varian Gemini 300 instrument (¹H, 300.1; ¹³C, 75.5 MHz), while the two-dimensional heterocorrelated (¹H–¹³C gHSQC, gHMBC experiments) spectra were recorded using a Varian Mercury-VX 400 (¹H, 399.8; ¹³C, 100.6 MHz) or Unity Inova-600 (¹H, 600.0; ¹³C, 150.9 MHz). The spectra were referenced internally to the residual solvent resonances and generally recorded at room temperature (298 K), unless otherwise reported. Solutions of the compound **8**_a at concentrations of 0.5–40 mM were used for NMR H-bond analyses. One-dimensional ¹H NMR spectra for determining temperature coefficients were obtained at 203–300 K in increments of 10 K. Electron impact mass spectra were taken on a VG 7070E mass spectrometer. Electrospray mass spectra were recorded on a Waters ZQ-4000 spectrometer. Elemental analyses were performed only on the air-stable salts or neutral species by using a CHNSO CE Instruments FLASH EA 1112 series. The composition of the reaction mixture is evaluated by mixture aliquots, detected by GC analyses and comparatively by GC-MS. Gas chromatography and GC-MS were performed on a HP6890 equipped with a 30 m × 0.2 mm Agilent DB-5 capillary column. General temperature program: 40 °C for 3 min, then 15 °C/min to 260 °C, which was maintained for 10 min. The general temperature program was able to separate all compounds. The reagent Re(CO)₅Br was prepared according to the literature procedure.³⁴ Pretreated γ -alumina (3% in H₂O w/w) and silica (230–400 mesh) gel (Aldrich) were heated under vacuum and cooled under nitrogen to room temperature. Column chromatography was performed under slight positive pressure. Solvent ratios are described as volumes before mixing. Cyclopentadiene (CpH) is from Aldrich Chemical Co. and was used without further purification. Indene (IndH) was purified by filtration over silica gel. Fluorene (FluH) was recrystallized from dichloromethane.

The aromatic alkaline salts NaCp,³⁵ NaInd,¹⁹ and LiFlu^{5e} were prepared as reported in the literature. The epoxides (**a** propylene, **b** styrene, **c** cyclopentene, oxides) are from Aldrich Chemical Co. and were used without further purification. The syntheses of ligands have been performed at the temperature specified in each case, until the disappearance of the starting material (checked by GC). The attribution of ¹H NMR signals relative to the side-chain diastereotopic CH₂H₁ methylene group may be inverted. Abbreviations: THF, tetrahydrofuran; MeCN, acetonitrile; ¹Pr, isopropyl; Ep, petroleum ether; GC, gas chromatography; GC-MS, gas chromatography–mass spectroscopy.

X-ray Crystallographic Study. Crystal data and collection details for HFlu_a^{OH}, **8**_a, are reported in Table 1. The diffraction experiments were carried out on a Bruker APEX II diffractometer equipped with a CCD detector using Mo K α radiation. Data were corrected for Lorentz polarization and absorption

(31) (a) Te Velde, G.; Bickelhaupt, F. M.; van Gisbergen, S. J. A.; Fonseca Guerra, C.; Baerends, E. J.; Snijders, J. G.; Ziegler, T. *J. Comput. Chem.* **2001**, *22*, 931–967. (b) *ADF2008.01, SCM, Theoretical Chemistry*; Vrije Universiteit: Amsterdam, The Netherlands, http://www.scm.com. (c) Jensen, F. *Introduction to Computational Chemistry*; Wiley: Chichester, 1999. (d) Klamt, A. *J. Phys. Chem.* **1995**, *99*, 2224.

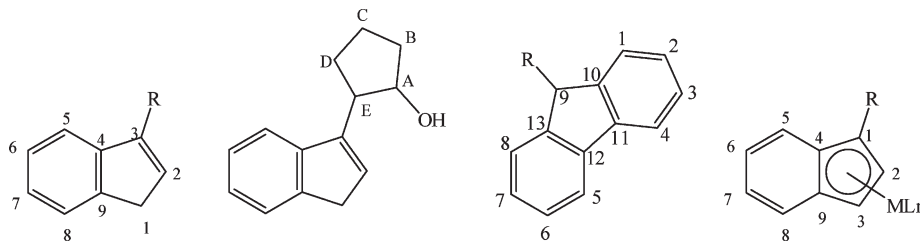
(32) (a) Becke, A. D. *Phys. Rev. A* **1988**, *38*, 3098–3100. (b) Lee, T.; Yang, W. T.; Parr, R. G. *Phys. Rev. B* **1988**, *37*, 785–789.

(33) Perrin D. D.; Armarego W. L. F.; Perrin D. R. *Purification of Laboratory Chemicals*, 2nd ed.; Pergamon Press: New York, 1980.

(34) Herrmann W. A. *Synthetic Methods of Inorganic Chemistry*; Georg Thieme Verlag: Stuttgart, 1997; Vol. 7.

(35) Panda, T. K.; Gamer, M. T.; Reosky, P. W. *Organometallics* **2003**, *22*, 877.

Chart 2. Numbering of the Carbon Atoms of Indenyl and Fluorenyl Ligands and Metal Complexes



effects (empirical absorption correction with SADABS).³⁶ Structures were solved by direct methods and refined by full-matrix least-squares based on all data using F^2 .³⁷ The asymmetric unit contains two independent molecules with identical connectivities, absolute S configuration at the quaternary asymmetric carbons [C(2) and C(22), respectively], and very similar bonding parameters. Hydrogen atoms bonded to carbon atoms were fixed at calculated positions and refined by a riding model. The H-atoms bonded to O-atoms in both the independent molecules were located in the Fourier map and refined isotropically with restrained O–H distances [0.84 Å, SE 0.02].

General Procedure for the Synthesis of Indenyl Alcoholate Derivatives 1_x ($x = a-d$), HInd_x^{O} . Epoxides a, b, c (10 mmol) were added at room temperature to freshly IndNa (10 mmol) in THF (50 mL). The resulting solution was stirred for 7 h in the case of propylene oxide a , for 7 h at reflux in the case of styrene oxide b , and for 24 h in the case of cyclopentene oxide c until the disappearance of starting material (monitored by GC). All volatiles were removed *in vacuo* to yield a red-brown air-sensitive powder containing alcoholate derivatives.

1_a , HInd_a^{O} : yield 98%. $^1\text{H NMR}$ (300 MHz, THF- d_8 , δ): 1.20 (d, 3H, $J_{\text{HH}} = 6.9$ Hz; Me), 2.51 (m, br, 1H, CH_aH_b), 2.8 (m br, 1H, CH_aH_b), 3.35 (s, 2H, CH_2 ring), 4.30 (m br, 1H, CH-O^-), 6.26 (s, 1H, H2), 7.1–7.6 (m, 4H). $^{13}\text{C}\{^1\text{H}\}$ NMR (75.44 MHz, THF- d_8 , δ): 27.6 (Me), 39.5 (CH_2 ring), 44.5 (CH_2), 69.4 (CHO), 121.2 (C5), 125.3 (C6), 126.0 (C7), 127.6 (C8), 129.8 (C2), 146.5 (C3), 146.5 (C9), 148.5 (C4).

1_b , HInd_b^{O} : yield 75%. $^1\text{H NMR}$ (300 MHz, THF- d_8 , δ): 2.871 (m, br, 1H, CH_aH_b), 3.207 (m, br, 1H, CH_aH_b), 3.264 (s, 2H, CH_2 ring), 5.334 (s, br, 1H, CH-O), 6.027 (s, 1H, H2), 7.20–7.60 (m, 10H). $^{13}\text{C}\{^1\text{H}\}$ NMR (75.44 MHz, THF- d_8 , δ): 39.5 (CH_2), 46.3 (CH_2 ring), 78.0 (CHO), 121.1 (C5), 125.2 (C6), 125.8 (C7), 127.1 (C8), 127.4 (*para*-CH Ph), 128.3 (*meta*-CH Ph), 129.0 (*ortho*-CH Ph), 130.9 (C2), 145.3 (C3), 146.3 (C9), 148.4 (C4), 154.7 (*ipso*-C Ph).

General Procedure for the Synthesis of Indene Ether $\text{HInd}_x^{\text{OMe}}$ ($x = a-d$). A 10 mL amount of methyl trifluoromethanesulfonate (1.13 mL, 10 mmol) in toluene solution was added, at -78°C via cannula, to relative alcoholate derivatives 1_{a-d} (10 mmol) in toluene (50 mL). The resulting reaction mixture was stirred at -78°C for 30 min and then warmed to room temperature until the parent alcoholate disappearance was detected by GC-MS. The yellow slurry was washed with aqueous NH_4Cl and the organic phase dried on MgSO_4 . After solvent removal the crude product was purified by column silica gel chromatography (70–230 mesh, grade 60) with Et_2O (95:5) to yield a pale yellow oil.

3_a , $\text{HInd}_a^{\text{OMe}}$: yield 98%. Anal. Calcd for $\text{C}_{13}\text{H}_{16}\text{O}$: C, 82.93; H, 8.57. Found: C, 82.90; H, 8.58. GC-MS (m/z (%)): 188 (10) $[\text{M}]^+$, 156 (24) $[\text{M} - (\text{MeOH})]^+$, 141 (12) $[\text{IndCHCH}_2]^+$, 128 (100) $[\text{IndCH}_2]^+$, 115 (19) $[\text{Ind}]^+$. $^1\text{H NMR}$ (300 MHz, CDCl_3 , δ): 1.14 (d, 3H, $J_{\text{HH}} = 6$ Hz; Me), 2.5 (m, 1H, CH_aH_b), 2.8 (m, 1H, CH_aH_b), 3.24 (s, 2H, CH_2 ring), 3.30 (s, 3H, OMe), 3.63 (m,

1H, CH-O), 6.19 (s, 1H, H2), 7.0–7.4 (m, 4H). $^{13}\text{C}\{^1\text{H}\}$ NMR (75.44 MHz, CDCl_3 , δ): 19.7 (Me), 35.0 (CH_2), 38.1 (CH_2 ring), 56.4 (OMe), 76.1 (CHO), 119.3 (C5), 124.0 (C6), 124.8 (C7), 126.3 (C8), 130.2 (C2), 141.5 (C3), 144.6 (C9), 145.7 (C4).

3_b , $\text{HInd}_b^{\text{OMe}}$: yield 75%. Anal. Calcd for $\text{C}_{18}\text{H}_{18}\text{O}$: C, 86.35; H, 7.25. Found: C, 86.30; H, 7.28. $^1\text{H NMR}$ (300 MHz, CDCl_3 , δ): 2.9–3.3 (m, 2H, CH_2), 3.356 (s, 3H, OMe), 3.401 (s, 2H, CH_2 ring), 4.65 (dd, 1H, CH-O), 6.31 (s, 1H, H2), 7.2–7.8 (m, 10H). $^{13}\text{C}\{^1\text{H}\}$ NMR (75.54 MHz, CDCl_3 , δ): 37.4, 38.4 (CH_2), 57.2 (OMe), 83.2 (CHO), 119.5 (C5), 124.2 (C6), 125.0 (C7), 126.5 (C8), 127.2 (*meta*-C Ph), 128.1 (*para*-C Ph), 128.9 (*ortho*-C Ph), 130.7 (C2), 141.2 (C3), 142.6 (C9), 144.7 (*ipso*-C Ph), 145.9 (C4).

3_c , $\text{HInd}_c^{\text{OMe}}$: yield 25%. Anal. Calcd for $\text{C}_{18}\text{H}_{18}\text{O}$: C, 86.35; H, 7.25. Found: C, 86.29; H, 7.29. $^1\text{H NMR}$ (300 MHz, CDCl_3 , δ): 3.358 (s, 3H, OMe), 3.504 (s, 2H, CH_2 ring), 3.96 (m, 1H, CH_aH_b), 4.10 (m, 1H, CH_aH_b), 4.44 (m, 1H, CHO), 6.31 (s, 1H, H2), 7.2–7.8 (m, Ph+Ind 9H). $^{13}\text{C}\{^1\text{H}\}$ NMR (75.44 MHz, CDCl_3 , δ): 38.4 (CH_2 ring), 45.3 (CHPh), 59.2 (OMe), 76.4 (CH_2O), 120.3 (C5), 124.1 (C6), 125.1 (C7), 126.4 (C8), 127.1 (*meta*-C Ph), 128.8 (*para*-C Ph), 128.9 (*ortho*-C Ph), 129.3 (C2), 141.2 (C3), 144.5 (C9), 144.7 (*ipso*-C Ph), 145.2 (C4).

3_d , $\text{HInd}_d^{\text{OMe}}$: yield 78%. Anal. Calcd for $\text{C}_{15}\text{H}_{18}\text{O}$: C, 84.06; H, 8.47. Found: C, 84.08; H, 8.49. $^1\text{H NMR}$ (300 MHz, CDCl_3 , δ): 1.70–1.89 (m, 6H, $\text{C}^3\text{H}_2 + \text{C}^4\text{H}_2 + \text{C}^5\text{H}_2$), 2.17 (m, 1H, C^2H), 3.35 (s, 3H, OMe), 3.9 (s, 2H, CH_2 ring), 4.35 (m, 1H, $\text{C}^1\text{H}\text{HO}$), 6.20 (s, 1H, H2), 7.17–7.49 (m, 4H). $^{13}\text{C}\{^1\text{H}\}$ NMR (75.44 MHz, CDCl_3 , δ): 23.9 (C^4H_2), 30.8 (C^3H_2), 31.9 (C^5H_2), 38.3 (CH_2 ring), 45.3 (C^2H), 57.5 (OMe), 87.5 (C^1HO), 120.3 (C5), 124.4 (C6), 125.2 (C7), 126.6 (C8), 127.2 (C2), 145.3 (C3), 145.8 (C9), 147.5 (C4).

General Procedure for the Synthesis of Indenyl Ether 4_{a-d} , $\text{LiInd}_x^{\text{OMe}}$ ($x = a-d$). A THF (40 mL) solution of the appropriate indene ether derivative 3_{a-d} (3.9 mmol) was cooled to -78°C and $n\text{-BuLi}$ (4.3 mmol, 1.1 equiv) added dropwise. The mixture was stirred for 1 h until room temperature was reached. The solution turned immediately from yellow to purple. The solvent was removed *in vacuo*, giving a red-brown solid.

4_b , $\text{LiInd}_b^{\text{OMe}}$: $^1\text{H NMR}$ (300 MHz, THF- d_8 , δ): 3.09 (s, 3H, OMe), 3.22–3.52 (m, 2H, CH_aH_b), 4.98 (d, 1H, $J_{\text{HH}} = 8.7$ Hz, CH-O), 6.08 (s, 1H, H2), 6.46 (s, 1H, H3), 6.63 (m, 4H, H5, H6, H7, H8), 7.20–7.90 (m, 5H, Ph). $^{13}\text{C}\{^1\text{H}\}$ NMR (75.44 MHz, THF- d_8 , δ): 41.3 (CH_2), 57.4 (OMe), 87.1 (CHO), 93.1 (C3), 114.8 (C5), 115.2 (C2), 117.1 (C6), 118.6 (C7), 121.2 (C8), 127.1, 128.3 (C4, C9), 128.7 (*meta*-C Ph), 129.4 (*para*-C Ph), 130.4 (*ortho*-C Ph), 132.8 (C3), 144.8 (*ipso*-C Ph).

General Procedure for the Synthesis of Sodium Cyclopentadienyl Alcohol Derivatives $\text{NaCp}_x^{\text{OH}}$ ($x = a-d$). Epoxide (A, B, 10 mmol) was added, via syringe, to a stirred solution of NaCp (0.88 g, 10 mmol) in THF (120 mL). The deep purple mixture was stirred at room temperature until the disappearance of starting material (monitored by TLC). The reaction color turned red brick in 4 h for 5_a and 17 h for $5_{b,c}$. The filtered solid was washed with diethyl ether (3×30 mL) to give a red-brown air-sensitive powder.

5_a , $\text{NaCp}_a^{\text{OH}}$: $\text{C}_8\text{H}_{11}\text{NaO}$. $^1\text{H NMR}$ (400 MHz, pyridine- d_5): 1.32 (s, br, 3H, Me), 2.70 (m, br 1H, CH_aH_b), 3.06 (m, br, 1H, CH_aH_b), 4.11 (m, br, 1H, CH-OH), 6.16 (s, br, 2H, H2, H5 Cp),

(36) Sheldrick, G. M. *SADABS, Program for Empirical Absorption Correction*; University of Göttingen: Germany, 1996.

(37) Sheldrick, G. M. *SHELXL97, Program for Crystal Structure Determination*; University of Göttingen: Germany, 1997.

6.30 (s, br, 2H, H3, H4 Cp). $^{13}\text{C}\{^1\text{H}\}$ NMR (100.59 MHz, pyridine-*d*₅): 24.7 (Me), 41.7 (CH₂), 70.0 (CHOH), 103.6, 105.0 (CHCp), 116.7 (*ipso*-C).

5_b, NaCp_b^{OH}: ^1H NMR (400 MHz, pyridine-*d*₅): 3.07 (m, 1H, CH_aH_b), 3.36 (m, 1H, CH_aH_b), 5.22 (m, 1H, CH-OH), 6.37 (s, br, 1H, H2 or H5 Cp), 6.43 (s, br, 2H, H3 + H4 Cp), 6.56 (s, br, 1H, H2 or H5 Cp), 7.22 (m, 1H, *para*-CH Ph), 7.33 (m, 2H, *ortho*-CH Ph), 7.64 (m, 2H, *meta*-CH Ph). $^{13}\text{C}\{^1\text{H}\}$ NMR (100.59 MHz, pyridine-*d*₅): 43.3 (CH₂), 76.8 (CHOH), 104.4 (C2, C5), 104.7 (C3, C4), 117.5 (*ipso*-Cp), 126.7 (*para*-C Ph), 126.9 (*meta*-C Ph), 128.7 (*ortho*-C Ph), 148.15 (*ipso*-C Ph).

5_c, NaCp_c^{OH}: ^1H NMR (400 MHz, pyridine-*d*₅): 3.6 (m, 1H, CHPh), 4.3 (m, 2H, CH₂O), 6.3–6.5 (m, br, 4H, Cp), 7.16 (s, 1H, *para*-CH Ph), 7.33 (m, 2H, *ortho*-CH Ph), 7.06 (m, 2H, *meta*-CH Ph). $^{13}\text{C}\{^1\text{H}\}$ NMR (100.59 MHz, pyridine-*d*₅): 52.5 (CHPh), 70.3 (CH₂O), 104.3 (CH Cp), 116.3 (*ipso*-C Cp), 125.6 (*para*-C Ph), 126.8 (*meta*-C Ph), 129.4 (*ortho*-C Ph), 147.0 (*ipso*-C Ph).

5_d, NaCp_d^{OH}: ^1H NMR (600 MHz, THF-*d*₈, δ): δ 6.72 (s, 2H, CH_{3,4}Cp), 6.14 (s, 2H, CH_{2,5}Cp), 4.55 (m, 1H, C_{1'}H-OH), 2.79 (m, 1H, C_{2'}H-Cp), 2.21, 1.67 (m, 6H, CH₂). $^{13}\text{C}\{^1\text{H}\}$ NMR (150.9 MHz, THF-*d*₈, 298 K): δ 126.45 (*ipso*-Cp), 113.2, 111.9, 109.7 (CHCp), 78.43 (C_{1'}H-OH), 37.15 (C_{2'}H-Cp), 31.34, 29.16, 21.23 (CH₂).

Reaction of Lithium Fluorene with Propylene Oxide. Racemic or enantiopure *S*-propylene oxide (10 mmol) was added at -78°C to a stirred solution in THF (50 mL) of FluLi (10 mmol). The resulting reaction mixture was stirred at -78°C for 30 min and then warmed to room temperature for 22 h, until disappearance of the fluorene (detected by GC-MS). The anionic orange mixture obtained consisted of an equimolar mixture of fluorene-propanolate **6_a** and fluorenyl-propanol **7_a** evaluated by NMR.

6_a, HFLu_a^{OLi}: ^1H NMR (400 MHz, THF-*d*₈, δ): 1.19 (d, 3H, $J_{\text{HH}} = 6\text{ Hz}$, Me), 1.85 (m, 1H, CH_aH_b), 2.23 (m, 1H, CH_aH_b), 4.16 (m, 1H, CH-O), 4.18 (m, 1H, CHR), 7.33–7.72 (m, 8H, arom). $^{13}\text{C}\{^1\text{H}\}$ NMR (100.59 MHz, THF-*d*₈, δ): 26.9 (Me), 40.6 (CHR), 46.1 (CH₂), 66.9 (CHO), 119.4, 119.7 (C1, C8), 123.4 (C5), 124.2 (C4), 126.8, 126.9 (C3, C6), 127.0, 127.1 (C2, C7), 141.4, 141.7 (C10, C13), 147.2, 147.9 (C11, C12).

7_a, LiFLu_a^{OH}: ^1H NMR (400 MHz, THF-*d*₈, δ): 1.34 (d, 3H, $J_{\text{HH}} = 6\text{ Hz}$, Me), 2.43 (m, 1H, CH_aH_b), 2.56 (m, 1H, CH_aH_b), 2.80 (s, br, 1H, OH), 4.83 (m, 1H, CHO), 6.85–8.52 (m, 8H, arom). $^{13}\text{C}\{^1\text{H}\}$ NMR (100.59 MHz, THF-*d*₈, δ): 23.5 (Me), 37.3 (CH₂), 69.7 (CHO), 90.2 (C9), 110.8 (C3, C6), 118.4 (C1, C8), 122.4 (C2, C7), 122.8 (C4, C5), 124.7 (C11, C12), 135.9 (C10, C13).

Neutralization of 6_a and 7_a to Fluorene Alcohol Derivatives. An ethereal solution containing **7_a** and **8_a** was washed with NH₄Cl(aq) (10 mL) and the organic phase dried overnight over MgSO₄. The solvent was removed *in vacuo*, yielding **9_a** as a waxy orange oil.

8_a, HFLu_a^{OH}: yield 95%. Anal. Calcd for C₁₆H₁₆O: C, 85.67; H, 7.14. Found: C, 85.34; H, 7.19. GC-MS (*m/z* (%)): 224 (14) [M]⁺, 206 (57) [M – OH]⁺, 191 (78) [FluCH₂CH]⁺, 178 (100) [FluCH₂]⁺, 165 (85) [Flu]⁺. ^1H NMR (600 MHz, CDCl₃, δ): 1.24 (d, 3H, $J_{\text{HH}} = 6.6\text{ Hz}$, Me), 1.90 (m, 1H, CH_aH_b), 1.99 (d, 1H, $J_{\text{HH}} = 3.6\text{ Hz}$, OH), 2.31 (m, 1H, CH_aH_b), 4.11 (m, 1H, CH-O), 4.22 (m, 1H, CHR), 7.38 (m, 2H, H3 + H6), 7.45 (t br, 2H, $J_{\text{HH}} = 7.8\text{ Hz}$, H2 + H7), 7.57 (d, 1H, $J_{\text{HH}} = 7.8\text{ Hz}$, H5), 7.68 (d, 1H, $J_{\text{HH}} = 7.8\text{ Hz}$, H4), 7.84 (m, 2H, $J_{\text{HH}} = 7.2\text{ Hz}$, H1 + H8). $^{13}\text{C}\{^1\text{H}\}$ NMR (100.59 MHz, CDCl₃, δ): 24.8 (Me), 43.3 (CH₂), 45.2 (C₉HR), 66.4 (CHO), 120.5, 120.6 (C1, C8), 124.9 (C5), 125.6 (C4), 127.2, 127.3 (C3, C6), 127.4, 127.5 (C2, C7), 141.3, 141.5 (C10, C13), 147.5, 148.0 (C11, C12).

Synthesis of HFLu_a^{OMe}, 9_a. Ligand **8_a** (10 mmol) was dissolved in Et₂O (70 mL). This solution was cooled to -30°C and treated with *n*-BuLi (11 mmol). This solution was stirred at 0°C for 2 h and added via cannula to a toluene solution (30 mL) of methyl trifluoromethanesulfonate (1.13 mL, 10 mmol) at -78°C . The resulting reaction mixture was warmed to room temperature for

5 h, until the parent alcoholate disappearance was detected by GC. The resulting yellow suspension was washed with aqueous NH₄Cl and the organic phase dried on MgSO₄. After solvent removal under reduced pressure, the crude product was purified by silica gel chromatography with Ep–Et₂O (95:5) to yield a pale yellow oil.

9_a, HFLu_a^{OMe}: yield 94%. Anal. Calcd for C₁₇H₁₈O: C, 85.67; H, 7.62. Found: C, 85.62; H, 7.69. GC-MS (*m/z* (%)): 238 (7) [M]⁺, 206 (92) [M – MeOH]⁺, 191 (100) [FluCH₂CH]⁺, 178 (36) [FluCH₂]⁺, 165 (71) [Flu]⁺. ^1H NMR (400 MHz, CDCl₃, δ): 1.09 (d, 3H, $J_{\text{HH}} = 6\text{ Hz}$, Me), 1.66 (m, 1H, CH_aH_b), 2.26 (m, 1H, CH_aH_b), 3.29 (s, 3H, OMe), 3.57 (m, 1H, CH-O), 4.11 (m, 1H, CHR), 7.20–7.80 (m, 8H). $^{13}\text{C}\{^1\text{H}\}$ NMR (100.59 MHz, CDCl₃, δ): 20.1 (Me), 41.8 (CH₂), 45.0 (CHR), 56.4 (OMe), 75.2 (CHO), 120.4, 120.5 (C1, C8), 125.0, 125.6 (C3, C6), 127.3, 127.4, 127.5 (C2, C4, C5, C7), 141.3, 141.6 (C10, C13), 148.0, 148.6 (C11, C12).

Synthesis of LiFLu_a^{OMe}, 10_a. The synthetic procedure was the same as described for **4_a** starting from fluorene derivative **9_a**.

10_a, LiFLu_a^{OMe}: ^1H NMR (400 MHz, THF-*d*₈, δ): 1.38 (d, 3H, $J_{\text{HH}} = 6\text{ Hz}$, Me), 3.22 (m, 1H, CH_aH_b), 3.55 (s, 3H, OMe), 3.63 (m, 1H, CH_aH_b), 4.02 (m, 1H, CHO), 6.67 (dd, 2H, $J_{\text{HH}} = 7.0\text{ Hz}$, $J_{\text{HH}} = 6.8\text{ Hz}$, H3, H6), 7.11 (dd, 2H, $J_{\text{HH}} = 8.0\text{ Hz}$, $J_{\text{HH}} = 6.8\text{ Hz}$, H2, H7), 7.55 (d, 2H, $J_{\text{HH}} = 8\text{ Hz}$, H1, H8), 8.13 (d, 2H, $J_{\text{HH}} = 7.6\text{ Hz}$, H4, H5). $^{13}\text{C}\{^1\text{H}\}$ NMR (100.59 MHz, THF-*d*₈, δ): 21.5 (Me), 35.6 (CH₂), 57.1 (OMe), 81.2 (CHO), 89.3 (C9), 109.6 (C3, C6), 115.2 (C1, C8), 120.3 (C2, C7), 120.9 (C4, C5), 123.6 (C11, C12), 136.8 (C10, C13).

Synthesis of Rhenium Alkoxide Derivatives 11_{a,b}, HInd_{a,b}^{ORe}(CO)₅. A THF (20 mL) solution of Re(CO)₅X (4.0 mmol) was added via syringe to a THF solution (25 mL) of the indene alcoholate (**1_{a,b}**) (4.2 mmol). The reaction mixture was stirred at room temperature for 2 h before being warmed to reflux temperature. The course of the reaction was monitored by IR spectroscopy until Re(CO)₅X disappeared. The obtained solid was washed with ethyl ether to extract the NaX (X = Cl, Br). No further workup was made to prevent decomposition of the desired products. Synthesis of **11_a** (X = Cl) requires 5 h, while 30 min was needed in the case of **11_b** (X = Br).

11_a, HInd_a^{ORe}(CO)₅: yield 1.898 g, 95%. Anal. Calcd for C₁₇H₁₃O₆Re: C, 40.80; H, 2.62. Found: C, 40.87; H, 2.59. IR (ν_{CO} THF): 2021 m, 1914 s, 1903 s, 1895 s cm⁻¹. ^1H NMR (300 MHz, CDCl₃, δ): 1.17 (d, 3H, $J_{\text{HH}} = 6\text{ Hz}$, Me), 2.61 (m, br, 2H, CH_aH_b), 3.22 (s, 2H, CH₂ ring), 4.06 (m, 1H, CHORe), 6.20 (s, 1H, H2), 7.05–7.40 (m, 4H). $^{13}\text{C}\{^1\text{H}\}$ NMR (75.44 MHz, CDCl₃, δ): 23.5 (Me), 38.1, 38.2 (CH₂), 66.9 (CHO), 119.4 (C5), 124.2 (C6), 125.1 (C7), 126.4 (C8), 130.8 (C2), 141.4 (C3), 144.7 (C9), 145.5 (C4), 193.5, 197.0 (CO).

11_b, HInd_b^{ORe}(CO)₅: yield 2.224 g, 99%. Anal. Calcd for C₂₂H₁₅O₆Re: C, 46.97; H, 2.69. Found: C, 47.01; H, 2.72. IR (ν_{CO} THF): 1999 m, 1885 vs. IR (ν_{CO} , KBr): 2109 w, 2018 s, 1979 m, 1900 vs cm⁻¹. ^1H NMR (600 MHz, THF-*d*₈, δ): 2.8 (m, br, 1H, CH_aH_b), 3.2 (m, br, 1H, CH_aH_b), 3.37 (s, 2H, CH₂ ring), 5.33 (s, br, 1H, CHO), 6.033 (s, 1H, H2), 7.10–7.70 (m, 10H). $^{13}\text{C}\{^1\text{H}\}$ NMR (75.44 MHz, THF-*d*₈, δ): 38.9 (CH₂ ring), 38.9 (CH₂), 73.8 (CHO), 120.4 (C5), 124.8 (C6), 125.6 (C7), 127.1 (*para*-C Ph), 127.3 (*meta*-C Ph), 128.1 (C8), 129.2 (*ortho*-C Ph), 131.6 (C2), 142.8 (C3), 145.7 (C9), 147.0 (C4), 154.5 (*ipso*-C Ph), 180.3, 187.7, 188.8, 199.8, 201.3 (CO).

Synthesis of 12_{a,d} and 13_{a,d} Derivatives. The appropriate ligand (**3_{a,d}**) (2.4 mmol) was dissolved in THF (10 mL) and deprotonated by dropwise addition of *n*-BuLi (2.5 mmol) at -78°C . This solution was stirred for 1 h at room temperature. The resulting purple anion (**4_{a,d}**) solution was cooled to -78°C and added via syringe to a THF solution (25 mL) of Re(CO)₅Br (0.8318 g, 2.05 mmol). The reaction mixture was stirred at -78°C for 30 min, before being warmed to room temperature. The reaction was monitored by IR in solution (THF). The reaction was stopped when the IR indicated the disappearance of Re(CO)₅Br (6 h for **4_a**, 3 h for **4_d**). Solvent was removed *in*

vacuo, and the resulting orange powder was extracted with diethyl ether (2 × 40 mL) and then chromatographed on silica gel (70–230 mesh, grade 60). Chromatography with Ep–Et₂O (1:1) gave a pale yellow fraction, namely, **13_a** or **13_d** followed by a yellow fraction corresponding to **12_a** or **12_d** by eluting with THF–Et₂O (1:1).

12_a, η^1 -**Ind_a**^{OMe}Re(CO)₅: yield 0.372 g, 35%. Anal. Calcd for C₁₈H₁₅O₆Re: C, 42.02; H, 2.94. Found: C, 42.05; H, 2.92. IR (ν_{CO} , CHCl₃): 2129 w, 2015 s, 1991 vs, 1979 vs, 1920 m cm⁻¹. ¹H NMR (300 MHz, CDCl₃, δ): 1.87 (d, 3H, $J_{\text{HH}} = 6$ Hz, Me), 2.6 (m, 1H, CHaHb), 2.9 (m, 1H, CHaHb), 3.2 (m, 1H, CHRe), 3.37 (s, 3H, OMe), 3.7 (m, 1H, CHO), 6.26 (s, 1H, H2), 7.0–7.6 (m, 4H, arom). ¹³C{¹H} NMR (75.44 MHz, CDCl₃, δ): 20.0 (Me), 35.4 (CH₂), 38.5 (CHRe), 56.8 (OMe), 76.5 (CHO), 119.6 (C5), 124.3 (C6), 125.1 (C7), 126.6 (C8), 130.6 (C2), 141.8 (C3), 144.9 (C9), 146.1 (C4), 187.2 (CO eq), 186.5 (CO ax).

12_b, η^1 -**Ind_d**^{OMe}Re(CO)₅: yield 0.476 g, 45%. Anal. Calcd for C₂₀H₁₇O₆Re: C, 44.44; H, 3.17. Found: C, 44.35; H, 3.21. IR (ν_{CO} , KBr): 2088 w, 2037 m, 1996 vs, 1893 m cm⁻¹. ¹H NMR (300 MHz, CD₃CN, δ): 1.20–1.50 (m, 6H, [CH₂]₃), 2.12 [m, 1H, C(E)H], 2.83 (t, 1H, CHRe), 3.27 (s, 3H, OMe), 4.28 (m, 1H, CHO), 5.16 (s, br, 1H, H2), 7.10–7.50 (m, 4H, arom). ¹³C{¹H} NMR (75.44 MHz, CD₃CN, δ): 22.0, 29.4, 34.2 (CH₂), 37.3 (CHRe), 44.4 (CHR), 56.2 (OMe), 86.6 (CHO), 119.6 (C5), 123.6 (C6), 124.4 (C7), 125.8 (C8), 126.6 (C2), 144.6 (C3), 145.2 (C9), 146.4 (C4), 178.5, 185.2, 189.7, 190.0, 196.7 (CO).

13_a, η^3 -**Ind_a**^{OMe}Re(CO)₄: yield 0.401 g, 40%. Anal. Calcd for C₁₇H₁₅O₅Re: C, 41.97; H, 3.11. Found: C, 41.88; H, 3.15. IR (ν_{CO} , CDCl₃): 2091 w, 1993 s, 1922 s, 1893 m cm⁻¹. ¹H NMR (300 MHz, CDCl₃, δ): 1.25 (d, 3H, $J_{\text{HH}} = 6$ Hz, Me), 2.7 (m, 1H, CHaHb), 2.8 (m, 1H, CHaHb), 3.41 (s, 3H, OMe), 3.8 (m, 1H, CHO), 6.7 (s, 1H, H3), 7.2–7.4 (m, 4H), 8.4 (d, 1H, $J_{\text{HH}} = 6.3$ Hz, H2). ¹³C{¹H} NMR (75.44 MHz, CDCl₃, δ): 20.1 (Me), 35.0 (CH₂), 56.5 (OMe), 69.1 (CHO), 118.5 (C5), 125.4 (C6), 126.0 (C7), 126.2 (C8), 132.4 (C3), 133.4 (C1), 144.9, 146.1 (C4, C9), 142.7 (C2), 185.0, 191.9, 192.6, 196.7 (CO).

13_d, η^3 -**Ind_d**^{OMe}Re(CO)₄: yield 0.424 g, 38%. Anal. Calcd for C₁₉H₁₇O₅Re: C, 44.53; H, 3.35. Found: C, 44.48; H, 3.39. IR (ν_{CO} , KBr): 2140 w, 1985 vs, 1915 s, 1856 m, sh cm⁻¹. ¹H NMR (300 MHz, CD₃CN, δ): 1.2–1.5 (m, 6H, [CH₂]₃), 2.7 [m, 1H, C(E)H], 3.31 (s, 3H, OMe), 3.93 (m, br, 1H, CHO), 6.69 (s, br, 1H, H3), 7.1–7.5 (m, 4H, arom), 8.5 (m, 1H, H2). ¹³C{¹H} NMR (75.44 MHz, CD₃CN, δ): 22.2, 26.0, 30.8 (CH₂), 44.3 [C(E)H], 56.3 (OMe), 87.1 (CHO), 119.5 (C5), 124.0 (C6), 124.5 (C7), 124.8 (C8), 127.2, 129.1 (C1, C3), 133.2, 136.82 (C4, C9), 142.3 (C2), 178.8, 187.5, 188.0, 200.8 (CO). ¹³C{¹H} NMR (75.44 MHz, C₆D₆, δ): 196.6, 193.7, 189.1, 179.0 (CO).

Degradation of 12_{a,d}, 13_{a,d} to Re₃(μ -H)₃(CO)₁₂: white microcrystalline solid. Anal. Calcd for C₁₂H₃O₁₂Re₃: C, 16.01; H, 0.33. Found: C, 15.99; H, 0.39. ESI-MS (MeCN, m/z (%)): 898 [M + H]⁺ (100). IR (ν_{CO} , Et₂O): 2046 s, 1984 m cm⁻¹. IR (ν_{CO} , KBr): 2154 w, 2063 s, 2033 vs, 1971 s, 1959 vs cm⁻¹. ¹H NMR (300 MHz, acetone-*d*₆): -17.0 s. ¹³C{¹H} NMR (75.44 MHz, acetone-*d*₆): 181.0, 205.2 (CO).

Synthesis of 14_b and Haptotropic Rearrangement to 16_b. To a THF (10 mL) solution of **3_b** (0.608 g, 2.43 mmol) cooled to -78 °C was added dropwise *n*-BuLi (1.0 mL of a 2.5 M solution in hexanes, 2.5 mmol, 1.04 equiv), and the mixture was stirred for 1 h until room temperature. The resulting purple solution was added to a THF solution (30 mL) of Re(CO)₃(MeCN)₂Br (0.7321 g, 2.024 mmol). The course of the reaction was monitored by IR spectroscopy until IR measurements indicated the disappearance of Re(CO)₃(MeCN)₂Br. Solvent was removed *in vacuo*, giving an orange-red solid. The crude product was extracted with diethyl ether (2 × 40 mL) to give an orange powder of **14_b**. During crystallization attempts of a MeCN/Et₂O mixture (-20 °C, 16 h) the color of the solution turned a deeper orange. The oily compound was treated with several extractions with toluene and filtered on a Celite pad. Solvent evaporation gave a waxy reddish compound. Spectroscopic measurements

(IR and NMR) reveal its transformation to **15_b**. Dissolution of **15_b** by CH₂Cl₂ caused prompt precipitation of a brown powder, which was extracted with toluene (3 × 10 mL). The residue was characterized by NMR spectroscopy, affording **16_b** (0.366 g, 34% yield calculated for **14_b**).

14_b, η^5 -**Ind_b**^{OMe}Re(CO)₃: yield 1.134 g, 90%. Anal. Calcd for C₂₁H₁₇O₄Re: C, 48.45; H, 3.29. Found: C, 48.50; H, 3.22. IR (ν_{CO} , KBr): 2020 s, 1899 vs, 1845 sh cm⁻¹. ¹H NMR (300 MHz, C₆D₆, δ): 3.19 (s, br, 3H, OMe), 3.28 (s, br, 2H, CH₂), 3.99 (m, br, 1H, CHO), 4.43 (m, 1H, H2), 4.56 (m, br, 1H, H3), 7.00–7.80 (m, 9H). ¹³C{¹H} NMR (75.44 MHz, C₆D₆, δ): 37.7 (CH₂), 57.1 (OMe), 79.6 (CHO), 83.8 (C3), 120.0 (C2), 124.6, 125.5, 126.9, 131.2 (CH Ind), 127.7, 129.2, 129.3 (CH Ph), 141.6, 142.9, 145.1 (*ipso*-C), 146.4 (*ipso*-C Ph), 192.6, 193.4, 193.8 (CO).

15_b, η^5 -**Ind_b**^{OMe}Re(CO)₂(NCMe): yield 0.442, 38%. Anal. Calcd for C₂₂H₂₀NO₃Re: C, 49.52; H, 3.78, N 2.63. Found: C, 49.48; H, 3.74, N 2.69. IR (ν_{CO} , toluene): 2036 m, 1908 vs cm⁻¹. IR (ν_{CO} , KBr): 2224 w (ν_{CN}), 2035 m, 1937 m, sh cm⁻¹. ¹H NMR (300 MHz, CD₃CN, δ): 1.92 (s, br, 3H, MeCN), 3.06–3.08 (m, br, 2H, CH₂), 3.24 (s, br, 3H, OMe), 4.0 (s, br, 1H, CHO), 4.2 (m, 1H, H2), 4.4 (m, br, 1H, H3), 7.0–7.80 (m, 9H). ¹³C{¹H} NMR (75.44 MHz, CD₃CN, δ): 5.1 (MeCN), 37.2 (CH₂), 57.2 (OMe), 81.9 (CHO), 84.0 (C3), 121.3 (MeCN), 122.9 (C2), 127.2, 127.4, 128.6, 129.1 (CH Ind), 129.3, 129.5, 129.75 (CH Ph), 142.8, 143.5, 144.5 (*ipso*-C), 146.9 (*ipso*-C Ph), 199.7, 201.0 (CO).

16_b, $\kappa^1\text{O}:\eta^5$ -**Ind_b**^{OMe}Re(CO)₂: yield 0.366 g, 90%. Anal. Calcd for C₂₀H₁₇O₃Re: C, 48.77; H, 3.48. Found: C, 48.81; H, 3.44. IR (ν_{CO} , KBr): 2014 m, 1895 vs cm⁻¹. IR (ν_{CO} , toluene): 2021 m, 1945 m cm⁻¹. ¹H NMR (300 MHz, CD₃CN, δ): 1.19 (s, br, 3H, OMe), 2.20 (s, br, 1H, CHO), 2.78 (s, br, 2H, CH₂), 3.7 (m, br, 1H, H2 + H3), 6.8–7.80 (m, 9H). ¹³C{¹H} NMR (75.44 MHz, CD₃CN, δ): 21.7 (OMe), 56.8 (CHO), 59.5 (CH₂), 72.1 (C3), 119.5 (C2), 127.7, 127.9, 128.1, 128.3 (CH Ind), 126.5, 129.4, 130.1 (CH Ph), 141.0, 142.2, 143.8 (*ipso*-C), 146.7 (*ipso*-C Ph), 192.3, 197.3 (CO).

Synthesis and Chelation of η^5 -Ind_c^{OMe}Re(CO)₃, 14_c. A THF solution of Re(CO)₃(MeCN)₂Br (0.7321 g, 2.51 mmol) was reacted with **LiInd_c**^{OMe} (**4**) prepared *in situ* (-78 °C) by addition of an equimolar amount of *n*-BuLi to derivative **3_c** (3.12 mmol, 1.24 equiv). Upon warming to room temperature the reaction went to completion in 4 h. Solvent was removed *in vacuo*, giving an orange-red solid, and the crude product was extracted with diethyl ether (2 × 40 mL) to give an orange powder of **14_c**. The rearrangement reaction was detected upon addition of THF at -20 °C for 6 h, by ¹H NMR monitoring. Solvent evaporation, filtering on a Celite pad, and washing with petroleum ether gave the oily **15_c**, which was characterized directly by spectroscopic means (IR, ¹H NMR). Dissolution of **15_c** by CH₂Cl₂ caused prompt precipitation of a brown-yellow powder, which was extracted by Et₂O. The residue was characterized by NMR spectroscopy, affording **16_c** (0.70 g, 60% yield calculated on **14_c**). Due to its low stability in solution, no ¹³C spectra could be recorded.

14_c, η^5 -**Ind_c**^{OMe}Re(CO)₃: yield 1.210 g, 93%. Anal. Calcd for C₂₁H₁₇O₄Re: C, 48.45; H, 3.29. Found: C, 48.43; H, 3.32. IR (ν_{CO} , THF): 2021 s, 1913 s, 1986 vs cm⁻¹. ¹H NMR (300 MHz, benzene-*d*₆, δ): 3.26 (s, br, 3H, OMe), 3.38 (s, br, 2H, CH₂), 4.12 (m, br, 1H, CHPh), 4.38 (m, 1H, H2), 4.63 (m, br, 1H, H3), 6.90–7.85 (m, 9H). ¹³C{¹H} NMR (75.44 MHz, benzene-*d*₆, δ): 44.4 (CHPh), 56.9 (OMe), 75.8 (CH₂), 84.0 (C3), 120.5 (C2), 124.4, 125.9, 127.2, 131.7 (CH Ind), 127.9, 129.5, 129.6 (CH Ph), 142.0, 143.1, 145.8 (*ipso*-C), 146.9 (*ipso*-C Ph), 187.3, 191.2, 192.4 (CO).

15_c, η^5 -**Ind_c**^{OMe}Re(CO)₂(THF): deep-orange oil. IR (ν_{CO} , THF): 2009 s, 1883 vs cm⁻¹. IR (ν_{CO} , cm⁻¹, KBr): 2017 s, 1904 vs. ¹H NMR (300 MHz, THF-*d*₈, δ): 1.73 (s, br, 4H, THF), 3.26 (m, br, 1H, CHPh), 3.28 (s, br, 3H, OMe), 3.36 (s, br, 1H, H3), 3.58 (s, br, 4H, THF), 3.8–3.9 (m, br, 2H, CH₂), 4.25 (m, br, 1H, H2), 6.8–7.5 (m, 9H).

16_c, $\kappa^1\text{O}:\eta^5\text{-Ind}_c^{\text{OMe}}\text{Re}(\text{CO})_2$: ochre waxy solid. Anal. Calcd for $\text{C}_{20}\text{H}_{17}\text{O}_3\text{Re}$: C, 48.77; H, 3.48. Found: C, 48.75; H, 3.51. IR (ν_{CO} , THF): 2021 s, 1915 s cm^{-1} . ^1H NMR (300 MHz, CD_2Cl_2 , δ): 1.11 (s, 3H, OMe), 2.75 (s, 1H, H2), 3.7 (m, 1H, *CHPh*), 3.4 (m, br, 3H, H3 + *CH*₂), 6.9–7.5 (m, 9H). $^{13}\text{C}\{^1\text{H}\}$ NMR (75.44 MHz, CD_2Cl_2 , δ): 22.7 (OMe), 44.1 (*CHPh*), 58.9 (*CH*₂), 75.7 (C3), 119.8 (C2), 124.0, 124.4, 125.5, 126.4 (*CH Ind*), 127.5, 128.5, 128.9 (*CH Ph*), 144.5 (*ipso-C Ph*), 140.0, 144.6, 147.4 (*ipso-C*), 193.5, 196.2 (CO).

Reaction of 5_a with $\text{Re}(\text{CO})_5\text{Br}$. Excess (4.0 mL, 4.6 mmol) **5_a** was added at rt via syringe to a THF solution (30 mL) of $\text{Re}(\text{CO})_5\text{Br}$ (0.513 g, 1.26 mmol) and stirred for 4 h. The crude product was extracted with Et_2O and dried under reduced pressure to give a white powder, identified as the known trihydroxy $\text{Na}[\text{Re}_2(\mu\text{-OH})_3(\text{CO})_6]$ complex. Yield: 0.224 g, 30%. Anal. Calcd for $\text{C}_6\text{H}_3\text{O}_9\text{Re}_2$: C, 12.14; H, 0.51. Found: C, 12.19; H, 0.62. IR (ν_{CO} , THF): 2004 vw, 1991 m, 1874 vs cm^{-1} .

Synthesis of 17_a, $\text{Cp}_a^{\text{OH}}\text{Re}(\text{CO})_3$. As alternative procedure, 1.5 equiv of anhydrous solid Me_3NO was added to the rhenium carbonyl bromide (0.506 g, 1.25 mmol) dissolved in 30 mL of THF. The mixture color turned in 1 h from bright violet to opalescent brown, while decarbonylation went to completion and $\text{Re}(\text{CO})_3(\text{THF})_2\text{Br}$ complex was formed *in situ*. A 2-fold excess of anionic ligand **5_a** was then added, and the reaction was monitored by IR spectroscopy for 2 h. The obtained brown solution after filtration over a Celite pad and extraction with diethyl ether was then chromatographed on an Al_2O_3 column. By elution with $\text{CH}_2\text{Cl}_2/\text{Ep}$ the collected fraction gave after solvent evaporation a yellow microcrystalline solid, which was identified as **17_a**.

17_a, $\text{Cp}_a^{\text{OH}}\text{Re}(\text{CO})_3$: yield 0.297 g, 60%. Anal. Calcd for $\text{C}_{11}\text{H}_{11}\text{O}_4\text{Re}$: C, 33.50; H, 2.81. Found: C, 33.56; H, 2.78. IR (ν_{CO} , CH_2Cl_2): 2006 m, 1887s cm^{-1} . ^1H NMR (400 MHz, CDCl_3 , δ): 1.12 (d, 3H, $J_{\text{HH}} = 6$ Hz, Me), 2.45–2.60 (m, 2H, *CH*₂), 4.05 (s br, 1H, OH), 4.38 (m, 1H, *CHO*), 5.27 (s, br, 2H, *CHCp*), 5.31 (s, br, 2H, *CHCp*). ^{13}C NMR (100.59 MHz): 23.7 (Me), 38.4 (*CH*₂), 69.9 (*CHO*), 84.5, 84.6, 84.9, 85.3 (*CH Cp*), 107.4 (*ipso-C*), 195.1 (CO).

Synthesis of 18_a, $\eta^1\text{-Flu}_a^{\text{OMe}}\text{Re}(\text{CO})_5$. A THF (10 mL) solution of methoxy-propyl fluorene derivative **9_a** (0.357 g, 1.5 mmol) was added dropwise at -78 °C to a hexane solution of *n*-BuLi (0.66 mL of a 2.5 M solution, 1.65 mmol, 1.1 equiv) and

stirred for 1 h until room temperature. The resulting purple **10_a** solution was then stirred with a THF solution (30 mL) of $\text{Re}(\text{CO})_5\text{Br}$ (0.518 g, 1.28 mmol) at -78 °C. The course of the reaction was monitored by IR spectroscopy, until disappearance of the starting carbonyl complex (20 h). Extraction of the crude product with diethyl ether (2×40 mL) indicated the formation of **19_a** as an orange-red powder. Thermal treatment of **18_a** gave rise to fast degradation to trimethoxy $\text{Na}[\text{Re}_2(\mu\text{-OMe})_3(\text{CO})_6]$, determined by comparison of its spectroscopic data. IR (ν_{CO} , CH_2Cl_2): 1989 s, 1872 vs cm^{-1} .

18_a, $\eta^1\text{-Flu}_a^{\text{OMe}}\text{Re}(\text{CO})_5$: yield 0.670 g, 92%. Anal. Calcd for $\text{C}_{22}\text{H}_{17}\text{O}_6\text{Re}$: C, 46.80; H, 3.04. Found: C, 46.86; H, 3.09. IR (ν_{CO} , THF): 2078 w, 2031 w, 1995 s, 1977 vs, 1953 m cm^{-1} . ESI-MS (MeOH; m/z (%)): 571 [$\text{M} + \text{H}$]⁺ (25), 515 [$\text{M} - 2\text{CO}$]⁺ (100). ^1H NMR (600 MHz, CDCl_3 , δ): 1.53 (d, 3H, $J_{\text{HH}} = 5.4$ Hz, Me), 2.82–2.84 (dt ABX, 2H, $J_{\text{HH}} = 4.2$ Hz, $J_{\text{HH}} = 3.0$ Hz, *CHaHb*), 4.15 (s, 3H, OMe), 4.69 (m, 1H, *CHO*), 7.30–8.0 (m, 8H, arom). $^{13}\text{C}\{^1\text{H}\}$ NMR (150.59 MHz, CDCl_3 , δ): 19.5 (Me), 41.6 (*CH*₂), 56.4 (OMe), 82.9 (C9), 92.9 (*CHO*), 120.5, 120.7, 121.7, 123.0, 123.6, 128.4, 128.9, 130.0 (*CH C1–C4*, *C5–C8*), 138.7, 140.1, 141.4, 141.6 (*ipso-C C11*, *C12*, *C10*, *C13*), 185.0, 186.2 (CO).

Acknowledgment. We thank the University of Bologna and the MIUR for supporting this work.

Supporting Information Available: ^1H NMR of **12_a** (Figure S1). ^1H NMR spectra of **10_a** (Figure S2). ^{13}C NMR spectra of **10_a** (Figure S3). Sample input for the ADF program (Table S1). X,Y,Z coordinates relative to DFT structure calculations *in vacuo* of the selected reported conformations, showing highest and lowest energy (Table S2). DFT frontier orbitals for **15_b** (Figure S4). DFT frontier orbitals for **15_c** (Figure S5). Experimental details on quenching of indenyl alcoholate derivatives **1_x** ($x = a\text{--}d$), HInd_x^{O} , to indenyl alcohol derivatives **2_x** ($x = a\text{--}d$), $\text{HInd}_x^{\text{OH}}$. Reaction of lithium indenide and propylene oxide. Reaction of lithium fluorenyl with styrene oxide. Synthesis of $\text{HFlu}_a^{\text{OLi}}$, **6_a**. Neutralization of fluorene derivatives. Selected bond lengths and angles for $\text{HFlu}_a^{\text{OH}}$, **8_a** (Table S2). This material is available free of charge via the Internet at <http://pubs.acs.org>.